CONTROLS ON ISOLATED CARBONATE PLATFORM EVOLUTION AND DEMISE, CENTRAL LUCONIA PROVINCE, SOUTH CHINA SEA

A Thesis

by

SERGIO OLAVE HOCES

Submitted to the Office of Graduate Studies of
Texas A&M University
in partial fulfillment of the requirements for the degree of

MASTER OF SCIENCE

August 2006

Major Subject: Geology

CONTROLS ON ISOLATED CARBONATE PLATFORM EVOLUTION AND DEMISE, CENTRAL LUCONIA PROVINCE, SOUTH CHINA SEA

A Thesis

by

SERGIO OLAVE HOCES

Submitted to the Office of Graduate Studies of
Texas A&M University
in partial fulfillment of the requirements for the degree of

MASTER OF SCIENCE

Approved by:

Chair of Committee,	Steven L. Dorobek
Committee Menbers,	Brian J. Willis
	Daulat Mamora
Head of Department,	Richard L. Carlson

August 2006

Major Subject: Geology

ABSTRACT

Controls on Isolated Carbonate Platform Evolution and Demise, Central Luconia Province, South China Sea. (August 2006)

Sergio Olave Hoces, B. S., Universidad Simón Bolívar

Chair of Advisory Committee: Dr. Steven L. Dorobek

Numerous isolated carbonate platforms developed in the Central Luconia Province of offshore Sarawak (during Middle to Late Miocene time). Fault-bounded highs produced largely by extensional deformation and later overprinted by strike-slip deformation provided substrates for the platforms and affected their growth histories. Flooding of these structural highs at ~16.5 Ma initiated carbonate sedimentation nearly simultaneously across the area. Later, third-order sea-level fluctuations and extrinsic factors such as differential subsidence, paleowind patterns and siliciclastic influx then controlled the internal architecture of the platforms. 2-D regional seismic lines, public-domain data and published literature were used to analyze growth patterns and demise of carbonate platforms across the study area.

Five Growth Stages were recognized in the carbonate platforms based on seismic facies analysis and stratigraphic relationships between reflectors. Platforms from the southeastern part of Central Luconia are thicker and larger than platforms located toward the central and northwestern areas, which reflect greater long-term tectonic subsidence to the southeast. Additionally, northwestward prograding siliciclastic sediments from

mainland Borneo caused additional flexural subsidence in the eastern part of the area and environmental deterioration for platforms located beyond the range of active siliciclastic sedimentation. Both of these factors reduced the growth potential of platforms and thus subdued carbonate development.

Platform termination was regionally diachronous and was produced in two steps. The first platforms drowned (~12.5-9.7 Ma) were in the eastern parts of the study area which were affected by incoming siliciclastic sediments and high local subsidence. Platforms drowned later (~6.3-5.5 Ma) were caused by a rapid sea-level rise combined with an intense local subsidence. Carbonate accumulation rates were measured between intraplatform markers, resulting in a trend that indicates a decrease in sedimentation rate with the square root of time.

Comparisons between Central Luconia carbonates and age-equivalent carbonate platforms elsewhere in East Natuna Basin showed that Central Luconia carbonate platforms were drowned earlier (latest late Miocene time) than East Natuna carbonate platforms (Early Pliocene time).

DEDICATION

To Marylena, for all her love and patient;

To Sergio and Natacha, for teaching me the highest family values;

To Carolina, for her unconditional support;

To Elsa, for lighting my way from heaven;

To Lucy, for all her love

ACKNOWLEDGEMENTS

I would like to express my sincere gratitude to Dr. S. L. Dorobek for accepting me as one of his students and allowing me to use his data. His knowledge and support have made my work possible and enjoyable.

My appreciation also goes to Dr. B. J. Willis and Dr. D. Mamora. I would like to thank them for their supervision and for serving as my committee members.

I am also thankful to the Department of Geology and Geophysics at TAMU, ConocoPhillips, and the American Association of Petroleum Geologist for scholarships and support.

Special thanks and gratitude to my friends Pablo, Rafael, Isaac, Gabriel, Fernando, Eduardo, Fady, Ezequiel, Yan, Hesham, Mike, Matt, and Coco for making my days at Texas A&M infinitely more enjoyable with exceptional grace, good humor and Northgate nights.

TABLE OF CONTENTS

Page

CHAPTER Page

LIST OF FIGURES

FIGURE Page

FIGURE Page

FIGURE Page

LIST OF TABLES

CHAPTER I

INTRODUCTION

Central Luconia Province is a broad continental shelf platform within Sarawak Basin (Figure 1), offshore Borneo, which is characterized by extensive development of Middle Miocene to Recent carbonate platform facies. Central Luconia is bounded to the west by the West Balingian Line, to the east by the West Baram Line, to the south by compressional/transpressional structures of the Balingian Province, and to the north by the North Luconia Province. Structurally, the Central Luconia Province is characterized by southwest to northeast trending fault-bounded basement highs and elongate troughs.

Seven major geological provinces have been identified in Sarawak Basin according to its structural and stratigraphic characteristics: SW Sarawak, West Luconia, Tatau, Balingian, Central Luconia, Tinjar, and the West and North Luconia Provinces (Figure 2). The Central Luconia Province displays a variety of structures in different parts of the basin. These are related to basement-involved extensional tectonics, strike-slip and wrench tectonics.

Although many carbonate platforms in Central Luconia Province have been buried by younger siliciclastic strata, some platforms are still growing in the northern part of this province. To date, more than 200 carbonate build-ups have been mapped over an area of 240 km by 240 km, with areal dimensions of a few to more than 200

This thesis follows the style and format of the American Association of Petroleum Geologists Bulletin.

km². Many platforms have been drilled and about twenty of them contain commercial quantities of non-associated gas. With more than 40 TSCF of gas initially in place and over 30 TSCF ultimate recovery, the Central Luconia Province represents about 40% of the total non-associated gas reserves in Malaysia.

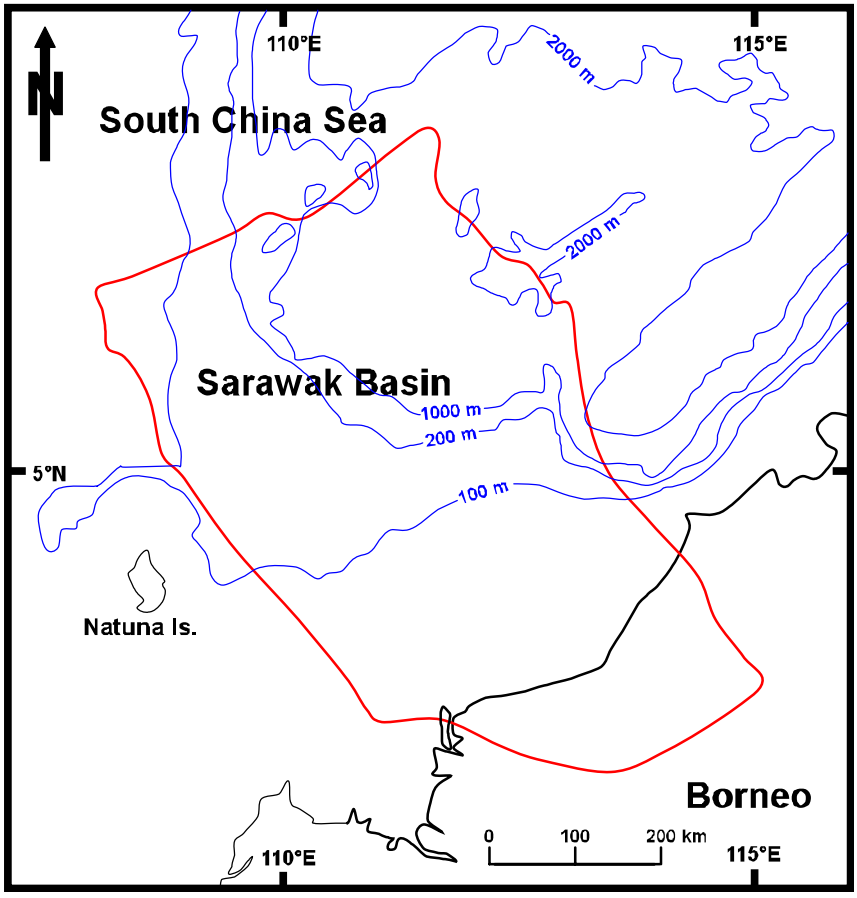

Figure 1. Sarawak Basin location. Limits of the basin (red line) defined by USGS.

During Late Oligocene to Early Miocene time the southern part of the Luconia Province was located in a coastal plain to inner neritic depositional setting (Ho, 1978), while the northern part of the province was characterized by inner to outer neritic facies.

The northern part of the province during this time was segmented into a series of south-southwest to north-northeast trending horst and graben structures created by numerous basement-involved normal faults, which affected carbonate platform growth. Later (Middle Miocene time), dextral strike-slip deformation overprinted the dominantly extensional setting and affected the internal stratigraphy of carbonate platforms that grew on fault-bounded highs.

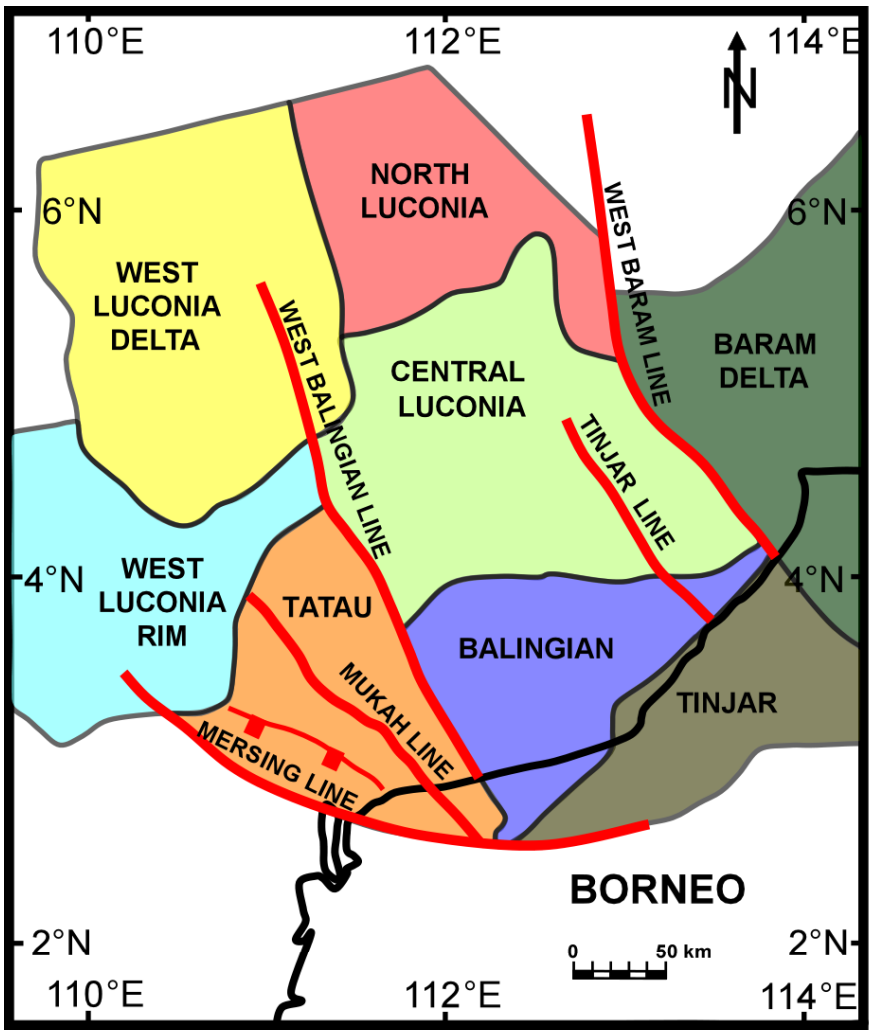

Figure 2. Sarawak Basin geological provinces (modified from Hutchison, 2005).

Carbonate deposition in the Central Luconia Province began during Early Miocene time, but was most prolific during Middle to Late Miocene time (Bracco Gartner et al., 2004). Successive stages of platform progradation, retrogradation and aggradation are recognizable on seismic profiles across the area.

Causes for platform termination in this area are poorly understood. Epting (1980, 1989) related platform termination to a relative sea-level rise that exceeded rates of carbonate production, whereas Vahrenkamp (1998) suggested that subaerial exposure caused by a sea-level fall terminated carbonate growth. Other workers (Fulthorpe and Schlanger, 1989; Zampetti et al., 2003) have suggested that platform termination was caused by a rapid sea level fall combined with an environmental stress produced by siliciclastic influx.

Although numerous gas reservoirs have been discovered within the Miocene carbonate platforms of the Central Luconia Province, and some of them have been analyzed in detail using high resolution 3D seismic data, well logs and core descriptions (Vahrenkamp, 1998; Zampetti et al., 2003, 2004; Bracco Gartner et al., 2004) little has been published about their regional geological evolution and stratigraphy.

The main objective of this project was to examine the geological evolution of Middle to Late Miocene carbonate platforms in the Central Luconia Province of offshore Sarawak (Figure 1). This involved the characterization of the different Growth Stages (aggradation, progradation, backstepping) of each carbonate platform by analyzing their internal seismic facies, stratal patterns and downlapping/onlapping relationships between carbonate platform-facies and siliciclastic facies that interfingered with and ultimately

buried the platforms. Factors that caused the demise of carbonate platforms in Central Luconia were also investigated.

CHAPTER II

METHODS

Regional structural and stratigraphic interpretations were completed for this project using PGS-Nopec's regional SEAS 95 "Supertie" seismic survey, which consists of over 10,000 line-kilometers of 2-D seismic reflection data (Figure 3). Seismic data were recorded to 6.0 to 8.0 seconds TWT (varies by seismic line), and consist of migrated and multifold seismic data. The survey includes coverage of offshore Vietnam, offshore NW Borneo and offshore Malaysia.

The SEAS-95 "Supertie" survey was loaded from tapes onto a UNIX workstation, and interpreted with aid of IESX, Basemap and CPS-3 modules of Schlumberger GeoFrame™ interpretation software.

Data from 32 wells located in adjacent basins were used to constrain the seismic interpretations. These well data typically included some check-shot data and several marker horizons corresponding to Miocene, Early Pliocene and Late Pliocene isochrons. Additional data (two well logs, lithologic description of a few wells and biostratigraphic markers from a short seismic section in Central Luconia Province) were taken from published work.

Internal seismic facies and stratal geometries of the platforms were recognized using seismic reflector termination patterns (onlap, downlap and erosional truncation), and lateral continuity and reflection-amplitude characteristics.

Time markers interpreted by Vahrenkamp et al. (2004) on a short segment of a regional 2-D seismic survey were used to constraint the ages within and above carbonate accumulations. These markers were correlated across the 2-D seismic profiles used during this study. Finer-scale internal carbonate stratal patterns were then related to the sea-level curve of Haq et al. (1988) (Figure 4).

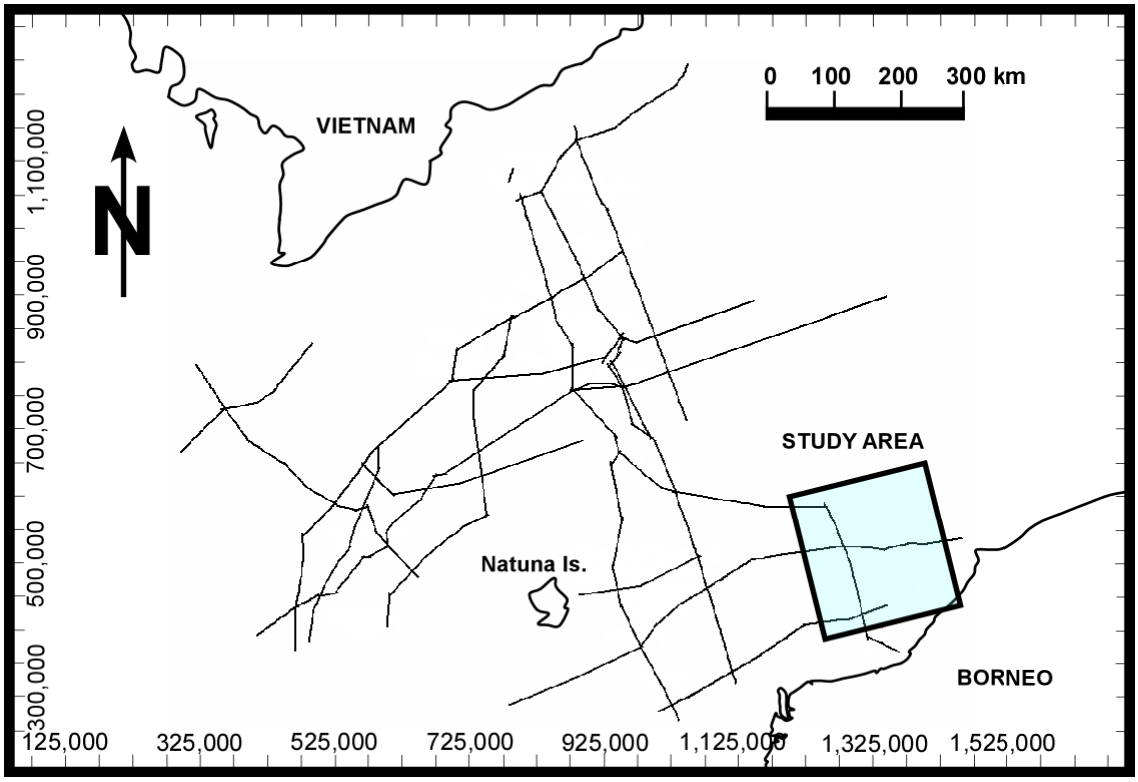

Figure 3. Coverage of SEAS 95 “Supertie” Seismic Survey.

Carbonate accumulation rates were calculated dividing the thickness (already converted to depth) measured between intraplatform markers by the time span elapsed (platform duration) between top and bottom markers.

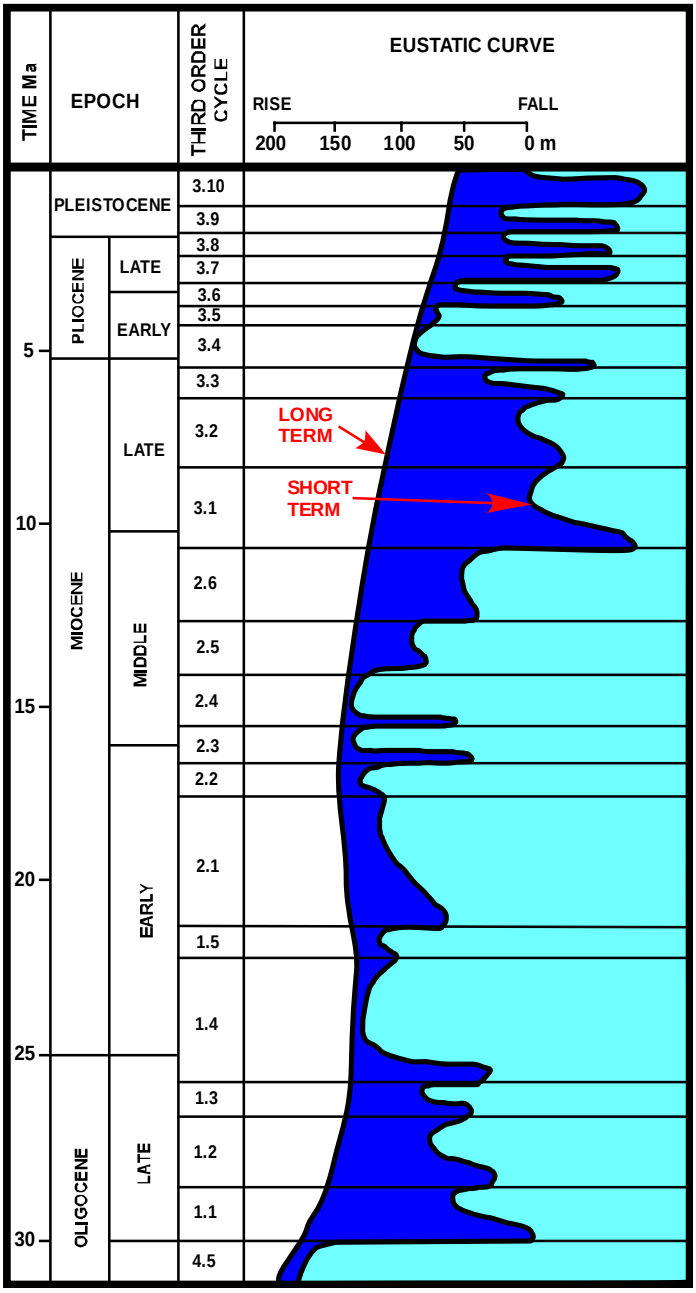

Figure 4. Eustatic sea-level change curve (after Haq et al., 1988).

Although data available for this study was a coarsely-spaced 2D seismic survey, general structural styles across the basin were recognizable and the main growth phases of the carbonate platforms could be defined using public-domain data and published

literature. Establishing 3-D facies relationships within platforms, however, was not possible using this type of data.

CHAPTER III

REGIONAL GEOLOGY OF SOUTHEAST ASIA

Southeast Asia continental crust is an amalgamation of continental fragments bounded by major fault zones, narrow mobile belts, or sutures that represent the sites of former subduction zones. Most continental fragments drifted away from Gondwanaland during Paleozoic and Mesozoic time (Metcalfe, 1996). In order to address in a better way the geological evolution of SE Asia, it is convenient at this point to divide the subject into a Pre-Tertiary phase and a Tertiary phase.

Pre-Tertiary Tectonic History of Southeast Asia

The Paleozoic and Mesozoic evolution of Southeast Asia involved three successive episodes (Devonian, late Early Permian and Late Triassic-Late Jurassic time) of rifting and separation of continental terranes from the northern margin of Gondwanaland, their northward drift and their amalgamation to form the proto Southeast Asian continent (Figure 5). The separation of these continental slivers was accompanied by the opening and subsequent closing of three ocean basins, the Paleo-Thetys, Meso-Thetys and Ceno-Thetys, remnants of which are now to be found along the various suture zones of Eastern Asia (Metcalfe, 1996).

Devonian rifting separated North China, South China, Indochina/EastMalaya /Qamdo-Simao, Tarim and Qaidam continental terranes from the northern part of Gondwanaland, forming the Palaeo-Thetys Ocean. A widespread Late Devonian to Early

Carboniferous unconformity is recognized on most of these blocks and may represent the breakup unconformity related to continental separation (Metcalfe, 1996). The Indochina and South China blocks (which once amalgamated is referred to as the Cathaysialand continent) are separated by a NW-SE oriented mobile belt where two sutures zones are recognized, the Song Ma and Song Da sutures of Paleozoic and Mesozoic age, respectively.

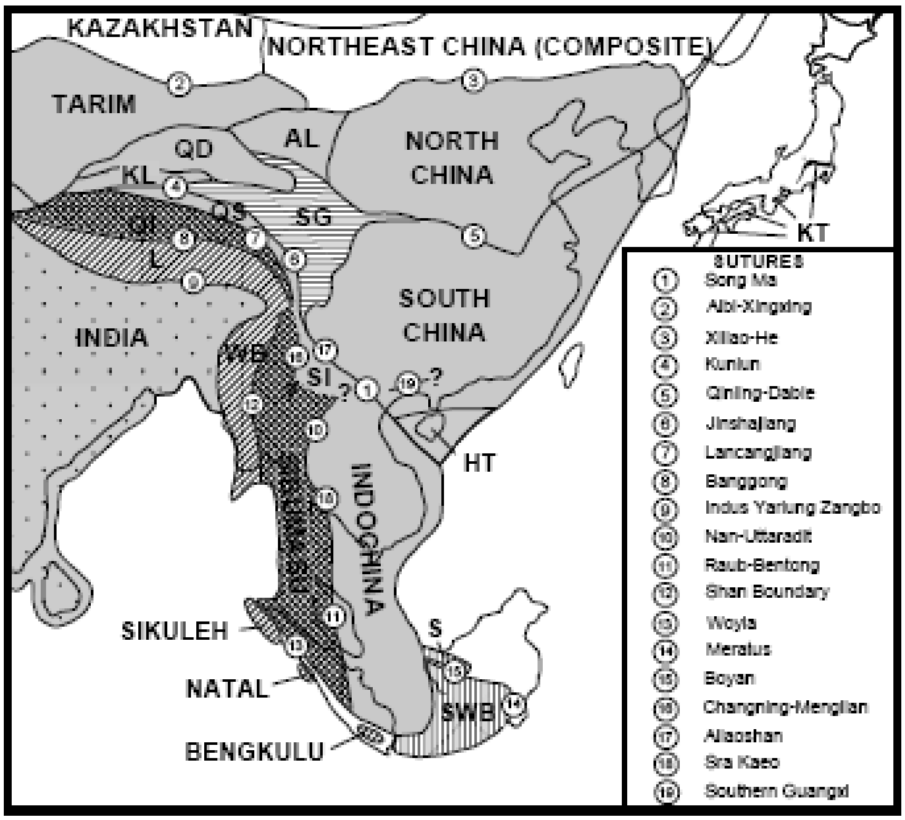

Figure 5. Principal accreted terranes and sutures of Southeast Asia (after Metcalfe, 1998). AL: Ala Shan Terrane; EM: East Malaysia; HT: Hainan Island Terrane; KL: Kunlan Terrane; L: Lhasa Terrane; QD: Qaidam Terrane; QS: Quamdo-Siamo Terrane; QT: Quiangtang Terrane; ST: Simao Terrane; S: Semitau Terrane; SG: Songpan Ganzi Accretionary Complex; SWB: Southwest Borneo; WB: West Burma.

A second episode of rifting occurred in the northern margin of Godwanaland during Carboniferous to Early Permian time, resulting in the separation of the Cimmerian continent (Sibumasu and Qiangtang continental blocks) from Gondwanaland and the opening of the Meso-Thetys Ocean. Suturing of Sibumasu and Qiangtang blocks to Cathaysialand occurred in Late Permian-Triassic time, closing a major branch of the Paleo-Thetys. The contiguous Nan-Uttaradit and Raub-Bentong suture zones represent the area where the Paleo-Thetys Ocean was subducted and ultimately resulted in continent-continent collision between Sibumasu and Indochina blocks.

The last episode of rifting occurred in Late Triassic to Late Jurassic time, where the Lhasa, West Burma and Woyla continental terranes separated from Godwanaland. The Lhasa block was rifted during Triassic time, and the Woyla and West Burma block did so during Late Jurassic time. The three blocks drifted northwards during Jurassic and Early Cretaceous time as the Ceno-Thetys Ocean was created and the Meso-Thetys was destroyed by subduction beneath Eurasia.

The SW Borneo and Semitau blocks, separated by the Boyan suture, were derived from the South China/Indochina margin by the opening of a marginal basin during Cretaceous time which was subsequently destroyed by southwards subduction when the South China Sea opened.

Tertiary Tectonic History of Southeast Asia

The main points discussed by geoscientists about the Tertiary tectonic evolution of Southeast Asia are the influence of the Indo-Asiatic collision, the rotation of Borneo,

and the spreading of the South China Sea in the formation of Cenozoic basins in the area. These aspects have been covered by Ben-Avraham and Uyeda (1973), Pupilli (1973), Molnar and Tapponnier (1975), Ben-Avraham (1978), Hamilton (1979), Taylor and Hayes (1980, 1982), Holloway (1982), Tapponnier et al. (1982), Ru and Pigott (1986), Daly et al. (1987, 1991), Peltzer and Tapponnier (1988), Hutchison (1989, 2004, 2005), Gower (1990), Lee and Lawver (1992, 1995), Briais et al. (1993), Packham (1993), Tongkul (1994), Hall (1996, 1997, 2002), Longley (1997), Wilson and Moss (1999) and Morley (2002).

Extrusion Model

The extrusion model (Figure 6) predicts that collision between India and Eurasia, which took place during Middle Eocene time (~45 Ma), caused lateral southeastward translation and clockwise rotation of Indochina and Sundaland through major strike-slip faults (Molnar and Tapponnier, 1975; Tapponnier et al., 1982; Peltzer and Tapponnier, 1988). It is inferred that the main faults that accommodated this lateral translation are the Red River, Three Pagodas, Ranong and Mae Ping Faults. There is still some debate as to the amount of displacement on these faults, especially on the Red River Fault, where the estimates of displacement range from 1,000-1,500 km (Tapponnier et al., 1986) to only 100 km (Rangin et al., 1995). Daly et al. (1987, 1991) mentioned that the very large displacements on strike-slip faults, predicted by Tapponnier et al. (1986), were geologically unproven.

The extrusion model explains satisfactorily existence of strike-slip faults across Indochina and Sundaland, seafloor spreading on the South China Sea and formation of Cenozoic basins across Indochina, Sundaland and the South China Sea.

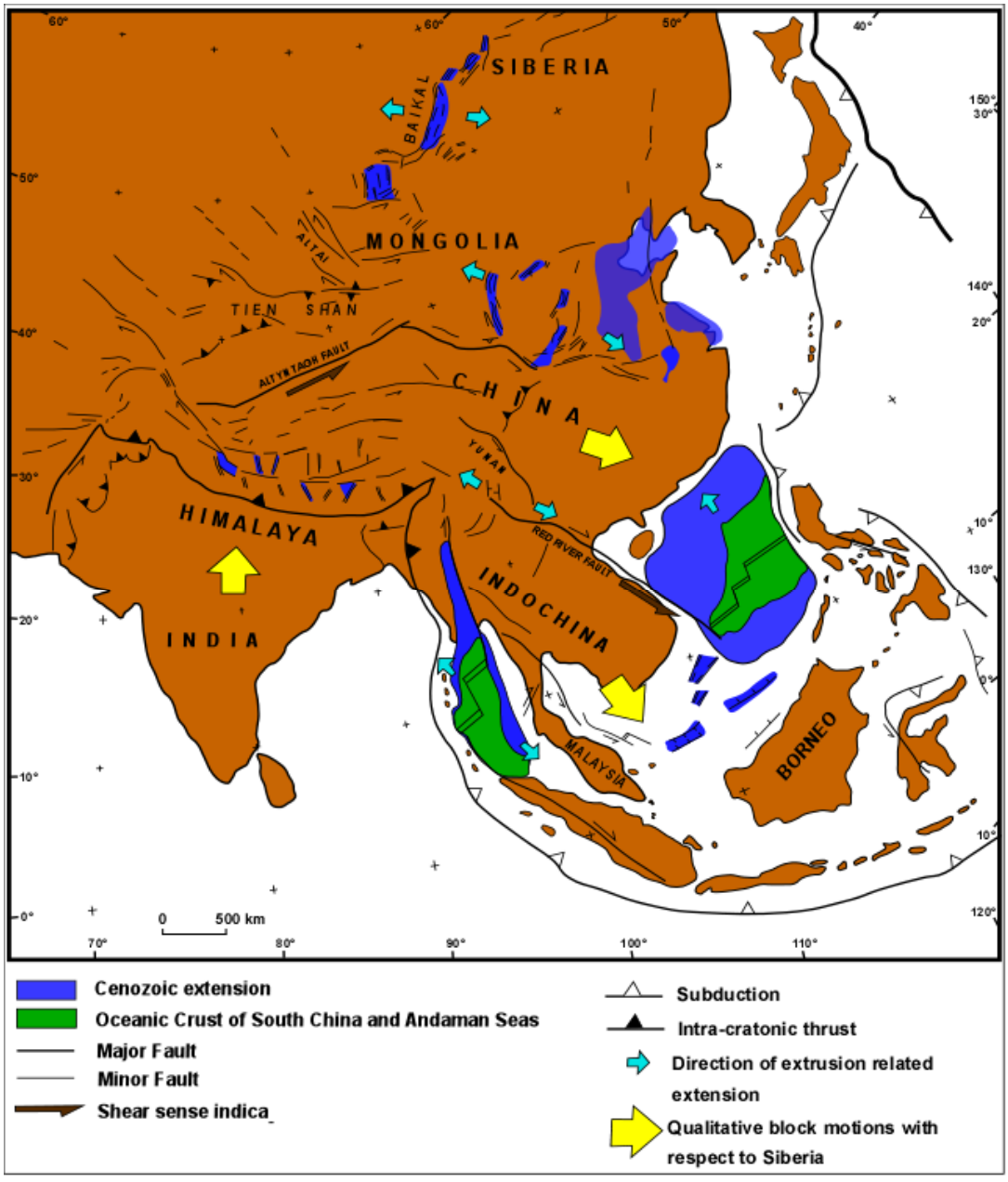

Figure 6. Extrusion Tectonic Model (after Tapponnier et al., 1982).

According to England and Molnar (1990), southeastward translation along strike-slip faults is an “illusion” and instead they suggested that the left-lateral slip on southeast striking planes is due to north-striking right-lateral simple shear. Daly et al. (1987, 1991) also argued that the assumption of Tapponnier et al. (1986) about a small component of N-S shortening in Tibet as a main support to postulate their model is wrong because the presence of extensive thrusting and N-S shortening in Tibet has been demonstrated through fieldwork.

Another points against the extrusion model are the fact that additional indentation experiments have not repeated the extensive lateral translation originally achieved (Daly et al., 1991), and the model proposed by Gower (1990), which suggests that Borneo and Malaya should be separate microplates during Early Tertiary time.

Seafloor Spreading in the South China Sea

South China Sea is an oceanic basin that includes an area around 1,500,000 km^2 of oceanic crust. It is bordered to the north by the broad China shelf, to the east by the Manila trench, to the west by the narrow Indochina shelf, and to the southeast by northwest Borneo and the Palawan Trough.

There has been some debate during the past years about the origin, evolution and driving mechanisms of seafloor spreading in the South China Sea. Karig (1971) proposed that the South China Sea Basin (SCSB) was produced as a result of a back-arc extension, which was in conflict with Ben-Avraham and Uyeda (1973), whose model for this region was based on east-west striking magnetic stripes (dated as Late Jurassic to

Early Cretaceous in age). Ben-Avraham and Uyeda postulated that Borneo was in a position next to mainland China and Hainan Island, and subsequently migrated southward during Jurassic time, producing the opening of the South China Sea (which had two subsequent periods of closing). Later, Ben-Avraham (1978) changed his interpretation about the age of opening of the SCSB and proposed a Cretaceous to Middle Miocene age for this episode.

Taylor and Hayes (1980) proposed that the SCSB is a small Atlantic-type marginal basin. According to them, SCSB opened between Middle Oligocene (~32 Ma) to late Early Miocene (~17 Ma) time based on the identification of east-west striking magnetic anomalies (11 to 5D) in the eastern part of the basin, which suggested a north-south direction of opening. They also postulated that the opening moved microcontinental blocks (North Palawan, Reed Bank and Luconia Shoals) southward from their original position in the southern part of mainland China to their current position offshore NW Borneo and Palawan (Ludwing et al., 1979). Later, Taylor and Hayes (1982) refined their interpretation using additional data and identified a relict spreading center trending southwest in the western half of the basin. They explained that this SW subbasin opened along a spreading center which propagated southwestward from the eastern subbasin in Early Miocene time. Seafloor spreading ceased shortly after the formation of the SW subbasin in Middle Miocene time when the microcontinental blocks collided with NW Borneo and Palawan, and shut down the southeastward subduction of the proto-South China Sea.

Although Holloway's (1982) conclusions were similar to those proposed by Taylor and Hayes (1980, 1982), he suggested that the spreading in the SW subbasin was coeval with spreading in the eastern part of the basin, in contrast to Taylor and Hayes's (1982) suggestion that the spreading center in the SW subbasin propagated southwestward from the eastern subbasin, with the spreading ceasing almost simultaneously.

Ru and Pigott (1986), based on heat flow, bathymetric data and backstripping, suggested that the SCSB has undergone three episodes of rifting (Late Cretaceous, Late Eocene and late Early Miocene) and two intervening stages of seafloor spreading since Early Cretaceous time. The age provided for the SW subbasin is significantly older (55 Ma) than the age provided for the eastern subbasin (17-32 Ma). Unlike Taylor and Hayes (1980, 1982), Ru and Pigott (1986) do not support an Atlantic-type origin for the SCSB.

Briais et al. (1989) proposed that the entire SCSB opened in a NW-SE direction and made no reference to episodic spreading events. However, Briais et al. (1993) refined their model by identifying anomalies 11 to 5c (32 to 16 Ma) and postulating an initial spreading between anomalies 11 and 7 (32 to 27 Ma) with a rate of ~5 cm/yr, and a subsequent SW spreading propagation with a decreased rate of ~3 cm/yr. The second episode of spreading was achieved by two southward ridge jumps at anomalies 6b-7 and 6 (Figure 7).

Lee and Lawver (1992, 1995) identified three stages of extension in the region. The first one, active during Late Cretaceous to Eocene time, produced the proto-South China Sea, which was consumed at the Palawan Trough following the southeastward

extrusion of Indochina. The second stage of extension formed the SCSB from north-south extension in the South China continental margin during Oligocene time. The third stage of extension occurred in early Miocene time, producing a NW-SE opening of the South China Sea Basin when the extrusion of Indochina was blocked by Sundaland.

Tongkul (1994) also suggested three episodes of spreading for the opening of the SCSB. The first related to the opening of the SW subbasin, the second related to both the opening of SW and eastern subbasins, and the third related to the opening of the eastern subbasin.

In contrast, Longley (1997) recognized two phases of spreading in the SCSB. The first one between 32 to 21 Ma, which was terminated by the Baram block collision with NW Borneo, and the second one between 21 to 11 Ma, that was terminated by the Palawan-Sulu block collision at ~11 Ma.

Pautot et al. (1990) studied the axial ridge of the SCSB using sea beam and single channel seismic profiles, magnetic and gravity profiles, rock dredges and sediment cores. They proposed two kinematic interpretations for SCSB evolution. One involves extrusion of Sundaland along major strike-slip faults in response to India-Eurasia collision (rifts trending NE-SW). The other interpretation suggests a 20º to 30º of counterclockwise rotation of the rift axis, implying a kinematic reorganization around ~20 Ma. Like Taylor and Hayes (1982), they postulated a synchronous cessation of spreading, but at ~16 Ma.

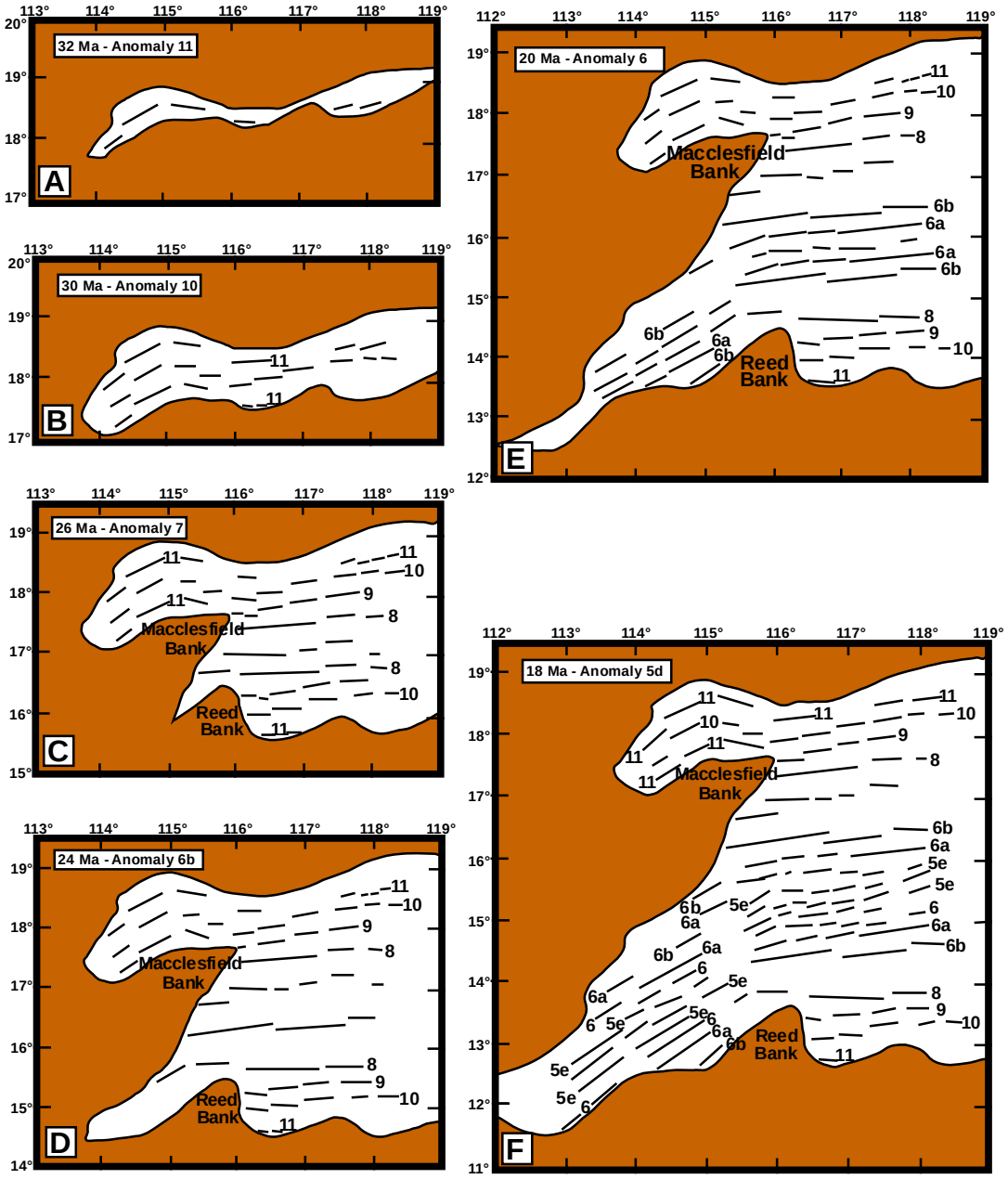

Figure 7. Different stages of seafloor spreading in the history of the South China Sea opening (after Briais et al., 1993).

There has been some controversy about driving forces that produced the opening of the SCSB. There is a group of workers that support the collision between India and

Eurasia as the driving mechanism (Molnar and Tapponnier, 1975; Tapponnier et al., 1982, 1986; Peltzer and Tapponnier, 1988; Briais et al., 1989, 1993; Lee and Lawver, 1992, 1995; LePichon, 1992; Huchon et al., 1994; Zhou et al., 1995). There is another group that suggests the SCSB opening was due to subduction-related extension (Fournier et al., 2004). A third group indicates back-arc extension due to subduction rollback is the driving mechanism (Daly et al., 1987, 1991). A fourth driving mechanism is postulated by Longley (1997), who suggested that SCSB opening is related to a plate reorganization at ~43.5 Ma. A fifth group, although recognizing the importance of strike-slip faults in Southeast Asia, favor motions of the Philippine Sea Plate and collision of the Australian Plate as driving mechanism for the SCSB opening (Hall, 1996; Wilson and Moss, 1999).

Borneo Rotation

Counterclockwise rotation of Borneo during middle to late Tertiary time is one of the unsolved issues in Cenozoic tectonic evolution of Southeast Asia. Its basement consists of Paleozoic and Mesozoic igneous, sedimentary and metamorphic rocks that behaved as a craton during most of Cenozoic time. To the north are younger additions to this continent, in the form of accretionary complexes and accreted terrains (Luconia Shoals, Reed Bank), related to southward subduction along the northern margin of Borneo (Hamilton, 1979).

Workers who advocate for a counterclockwise rotation of Borneo (Hamilton, 1979; Holloway, 1981; Taylor and Hayes, 1982; Daly et al., 1987, 1991; Fuller et al., 1991; Hall, 1996; Moss et al., 1997) based their interpretation on paleomagnetic data

from Cretaceous plutonic rocks sampled in western Borneo (Haile et al., 1977). More recent studies carried out by Schmidtke et al. (1990) also support an episode of rotation. Those workers that reject a rotation of Borneo (Rangin et al., 1990; Lumadyo et al., 1993; Lee and Lawver, 1994) argue that the data of Haile et al. (1977) were structurally uncorrected, and the data of Schmidtke et al. (1990) were sampled from a structurally complex area and allochthonous terrains. According to these workers, predicted rotation based on these data is not consistent with major Cenozoic structures in the region.

Sarawak Basin Tectonic Evolution

Sarawak Basin is located on the northern margin of NW Borneo and extends about 300 km offshore (Figure 1). The Basin transitions northward into deep-water parts of the South China Sea, is bounded to the south by Lower Tertiary and older sediments and basement rocks of Borneo, to the east by the West Baram Line (a prominent NW-SE trending fault zone), and to the west by the Sokang Trough.

During early stages of petroleum exploration in the area, many local stratigraphic units were created in order to describe the stratigraphy of offshore Sarawak. Many Tertiary formations were defined by paleontological methods due to the absence of distinctive lithological characteristics. Ho (1978) used wireline logs and well data to subdivide the Upper Eocene to Pleistocene sedimentary sequence into eight major cycles, separated by widespread flooding surfaces that partition the overall regressive package.

To set a comprehensive time-stratigraphic scheme, Ho (1978) used a combination of planktonic foraminiferal zonation for open marine environments, larger foraminiferal biostratigraphy for carbonate facies, and palynological zonation for fluvial to coastal deposits. In Ho's stratigraphic scheme for the Sarawak Basin, each cycle starts at a transgressive base overlain by a regressive sequence.

Mat-Zin (1996) identified seven unconformities within Tertiary strata of the Sarawak Basin. Where these unconformities transition laterally into conformable intervals, biostratigraphy and wireline log data were used to guide correlations. Mat-Zin (1996) and Mat-Zin and Swarbrick (1997) also established a regional correlation framework for Ho's eight major cycles, Hageman's cycles (Hageman, 1987), and Mat-Zin (1996) sequences for Sarawak Basin (Figure 7).

According to Mat-Zin (1996), the Sarawak Basin formed as a result of southwest-northeast, trending strike-slip faulting during Late Oligo-Miocene time, which created an earlier NW-SE coastline and divided offshore Sarawak area into Eastern and Northwestern sub-basins (Figure 8), where ~13 km (more than 6 seconds TWT) of sediments accumulated. These sub-basins are separated by a narrow basement high that is bounded by a pronounced structural lineament known as the West Balingian Line, one of several NW-SE trending lineaments within the Sarawak Basin. The Eastern sub-basin formed during Late Oligocene time and is characterized by coastal plain and shallow marine facies, whereas the Northwestern sub-basin is younger in age and remained structurally high until Late Miocene time.

Many dextral strike-slip faults in the Sarawak Basin are parallel to other major, NW-SE trending structural lineaments, such as the West Balingian Line, Mukah Line, Igan-Oya Line, Tinjar Line, and West Baram Line (Figure 9). These lineaments are actually complex fault zones that are characterized by variable fault throw and age along strike, and the timing of movements along them suggests a progressive younging toward the east. The latest fault displacements in the Baram Delta area (east of Sarawak Basin) occurred during Pliocene time (Mat-Zin, 1996; Mat-Zin and Swarbrick, 1997).

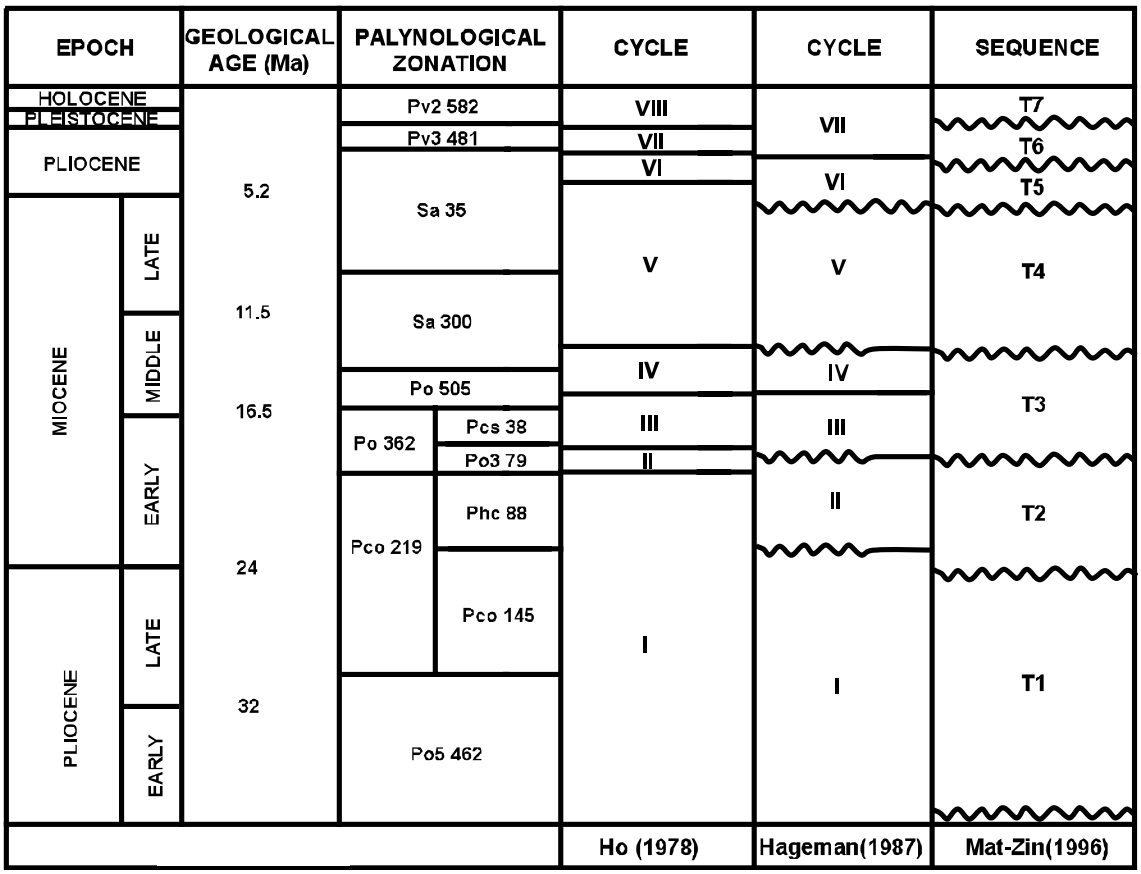

Figure 8. Stratigraphic scheme of Sarawak Basin over the years (After Mat-Zin, 1996).

These fault zones strongly influenced Tertiary stratigraphic development throughout the Sarawak Basin until Middle Miocene time, when regional tectonic subsidence across the basin became more dominant. The main structural features associated with these fault zones include negative flower structures, local fault inversion, and local evidence in the stratigraphy for both extension and compression throughout Cenozoic time.

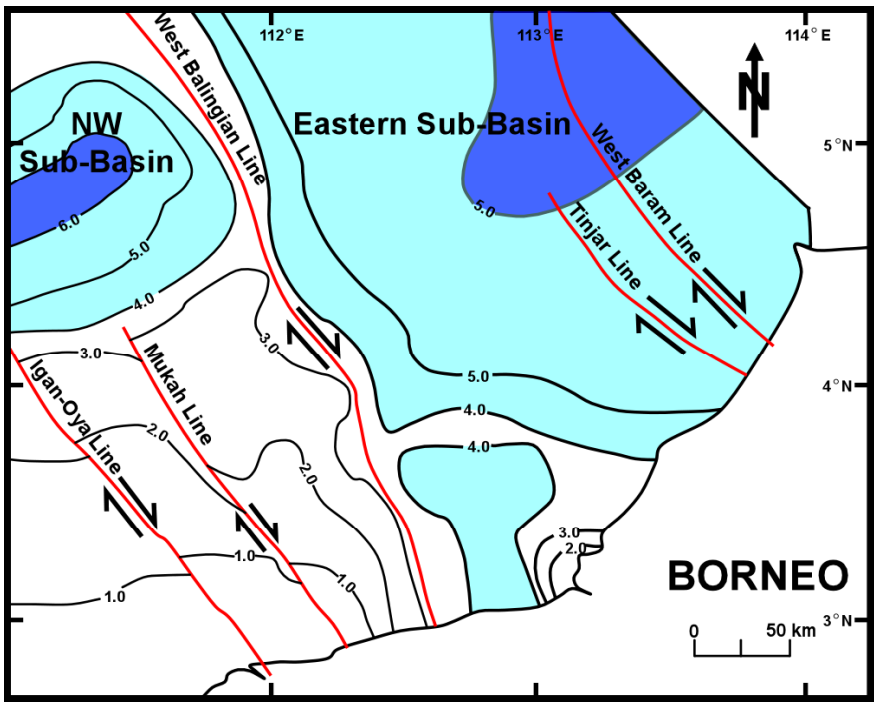

Figure 9. Major structural elements of Sarawak Basin (after Mat-Zin, 1996).

Central Luconia Province

Central Luconia is bounded to the west by the West Balingian Line, to the east by the West Baram Line, to the south by compressional/transpressional structures of the

Balingian Province, and to the north by the North Luconia Province (Figure 2). Structurally, the Central Luconia Province is characterized by southwest to northeast trending fault-bounded basement highs and elongated troughs (Epting, 1980; Hutchison, 1989).

Shallow marine carbonate platforms have developed across Central Luconia Province (Figure 10) since late Early Miocene time. Although many of these platforms have been buried by younger siliciclastic strata, some platforms are still growing in the northern part of this province.

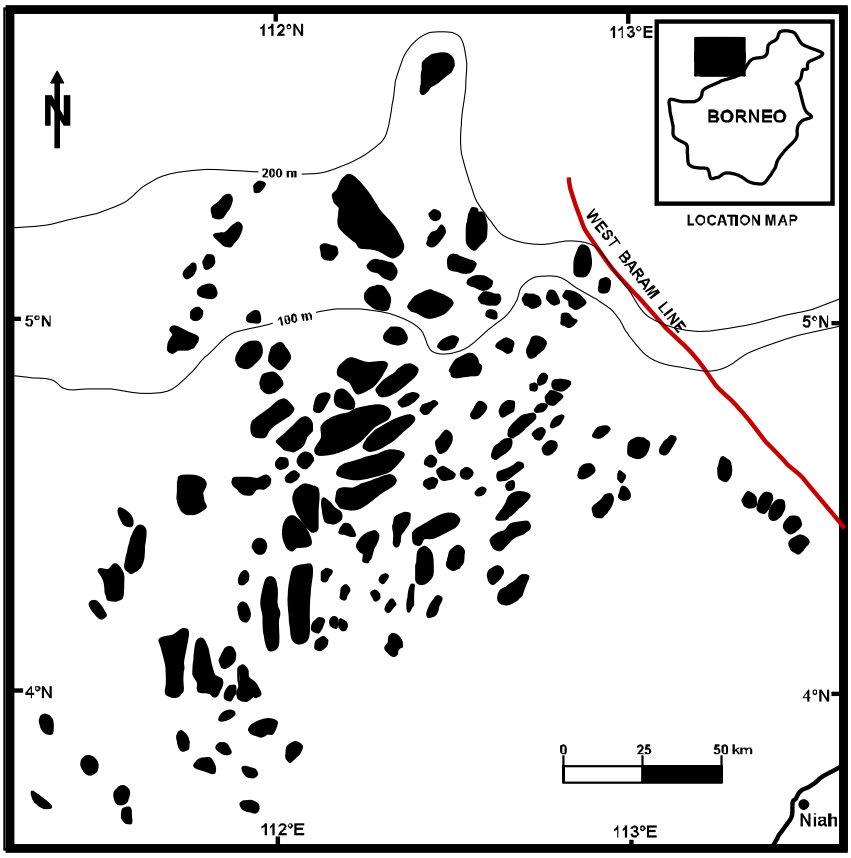

Figure 10. Distribution of Neogene carbonate platforms across the Central Luconia Province (modified from Epting, 1980).

Central Luconia Province was part of a microcontinental fragment that drifted southward from southern China toward Sundaland during Middle Oligocene to late Early Miocene and was subsequently docked on to the continental margin of Borneo during the subduction and subsequent collision that created the Rajang Belt in northern Borneo (Taylor and Hayes, 1982; Hutchison, 1989). However, Lee and Lawver (1992, 1995) and Wilson and Moss (1999) suggest, however, that Central Luconia Province was part of a NW-SE oriented shelf of Borneo.

CHAPTER IV

DATA DESCRIPTION AND INTERPRETATION

Carbonate platforms studied on this project are depicted in Figure 11, which also shows the basemap for the interpreted seismic sections, displaying two main regional lines (E-W and N-S trending profiles) that cover the study area. Seismic lines and platform location have been shifted ~10 km from their original locations in order to protect the proprietary character of the data.

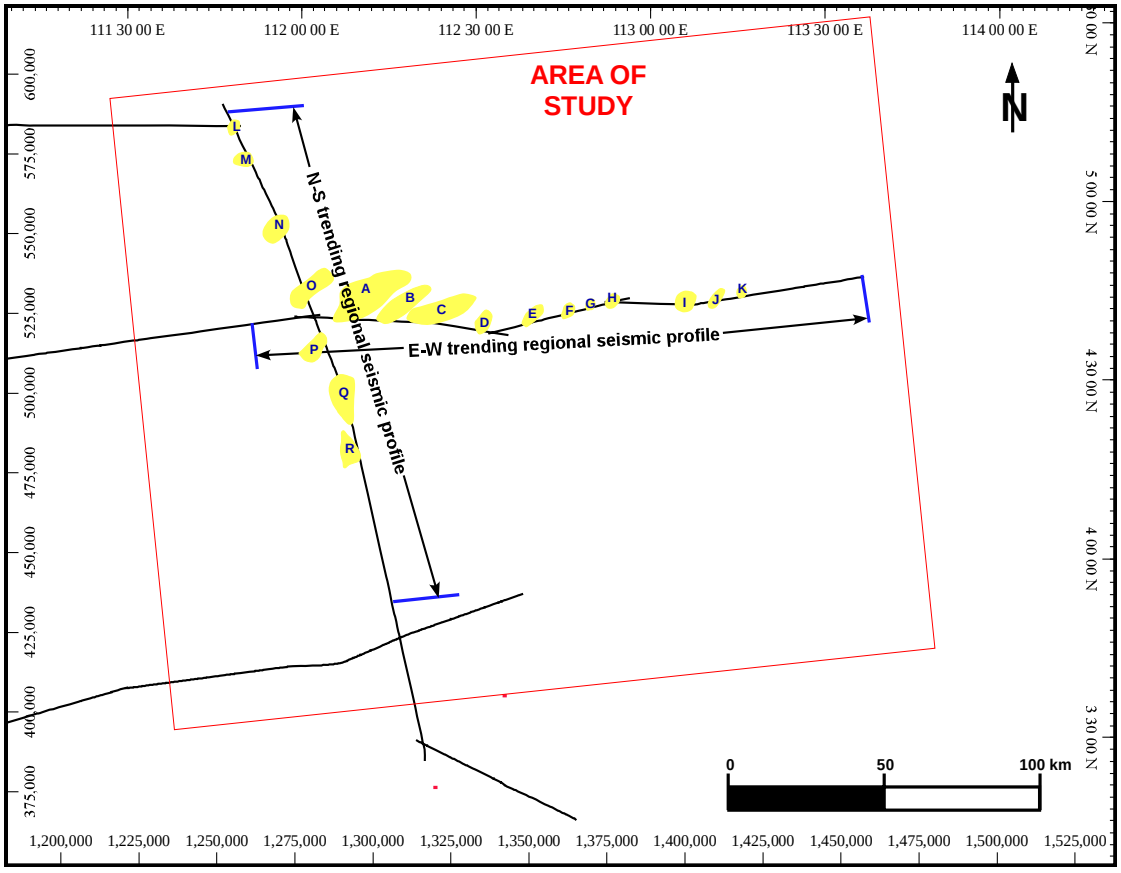

Figure 11. Distribution of carbonate platforms analyzed and seismic profiles interpreted.

Description

E-W Trending Profile

The E-W trending seismic profile (Figures 12 through 17) is ~195 km long and intersects eleven carbonate platforms located on tectonic highs produced by strike-slip deformation. From west to east the carbonate platforms were labeled: platform A-K.

Distances between carbonate platforms are used to define three groups. Platforms A, B and C in the western part of the study area are about 3 to 4 km apart. Platforms D, E, F, G and H, located in the central part of the seismic profile are 5 to 6 km apart. Platforms I, J and K, located in the eastern part of the seismic line, are ~3 km apart.

Carbonate platform thicknesses were measured in two-way travel time (Table 1) and then converted to depth (Table 2) using a constant velocity value of 4,000 m/s, which is the velocity value for carbonate rocks with an average porosity of approximately 25% (Vahrenkamp et al., 2004). Results indicate that platforms in the western part of the seismic line tend to be thicker (exceeding 1500 m) than platforms in the eastern part, where total carbonate thicknesses do not exceed 1400 m.

Table 1. Thicknesses (in miliseconds) of the different third-order cycles across the carbonate platforms measured over the E-W seismic profile.

Plat.	Cycle 2.3	Cycle 2.4	Cycle 2.5	Cycle 2.6	Cycle 3.1	Cycle 3.3	TOTAL(ms)
A	110	108	78	146	226	22	690
B	106	97	98	165	244	28	738
C	150	82	90	146	161	117	746
D	112	80	132	166	154	106	750
E	132	98	144	145	258	Terminated	777
F	78	98	156	258	Terminated	Terminated	590
G	109	86	123	123	Terminated	Terminated	441
H	120	158	108	124	152	Terminated	662
I	202	80	232	78	54	Terminated	646

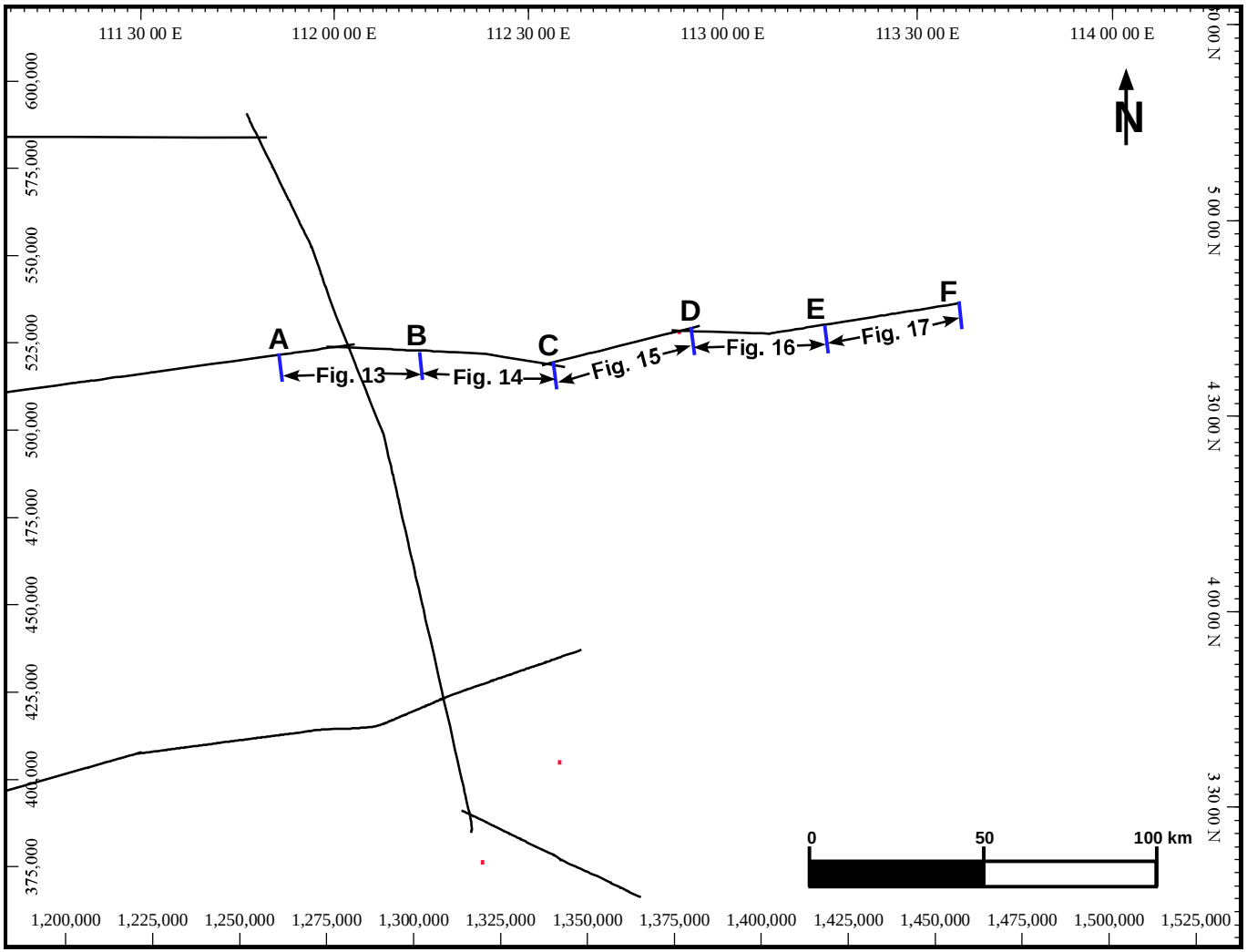

Figure 12. Location of E-W seismic profiles used for this study (from the SEAS 95 “Supertie” Seismic Survey).

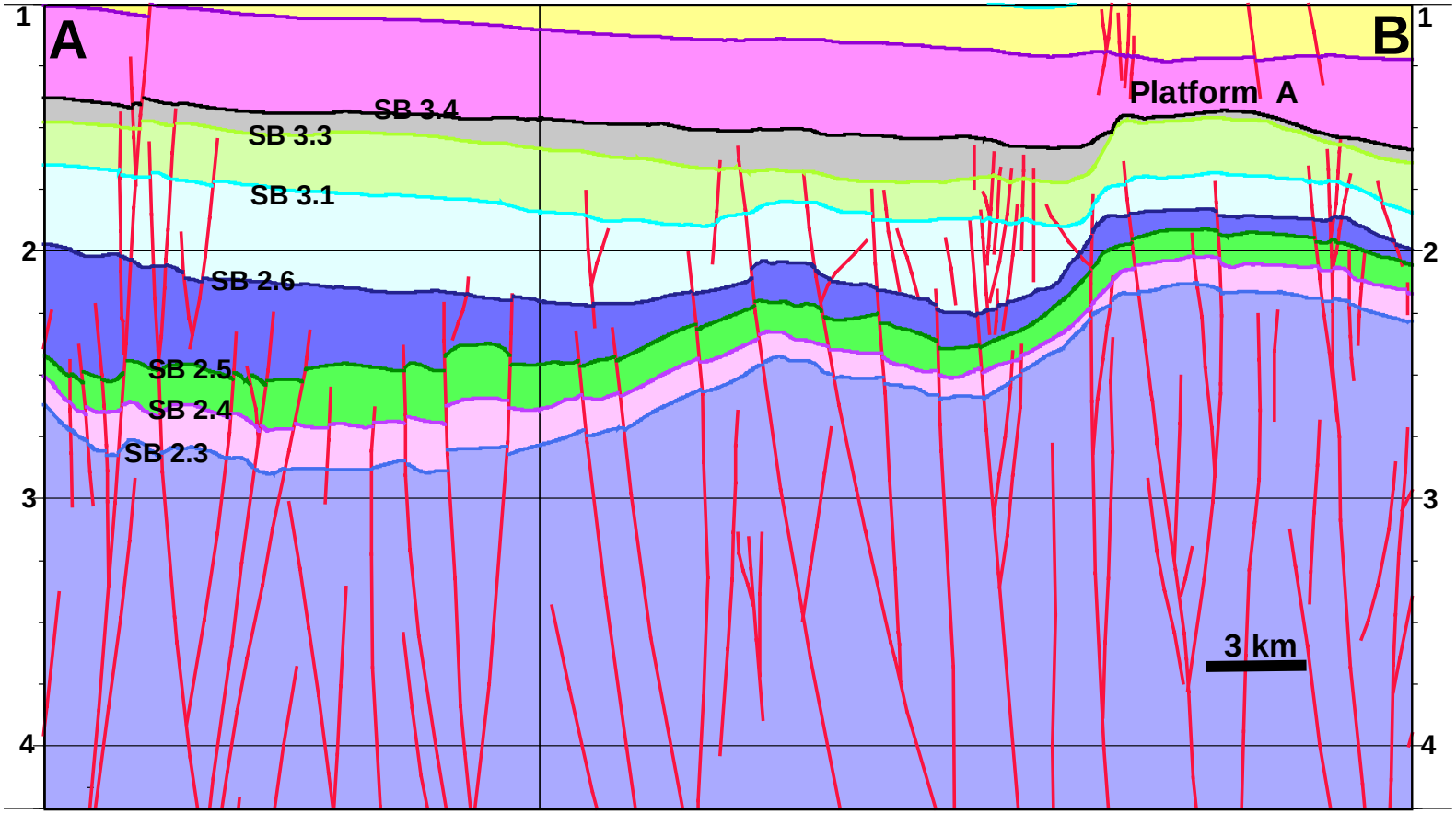

Figure 13. Interpretation from seismic profile A-B (see Figure 12 for line location). The figure shows Platform A. Farther west there are no carbonate platforms.

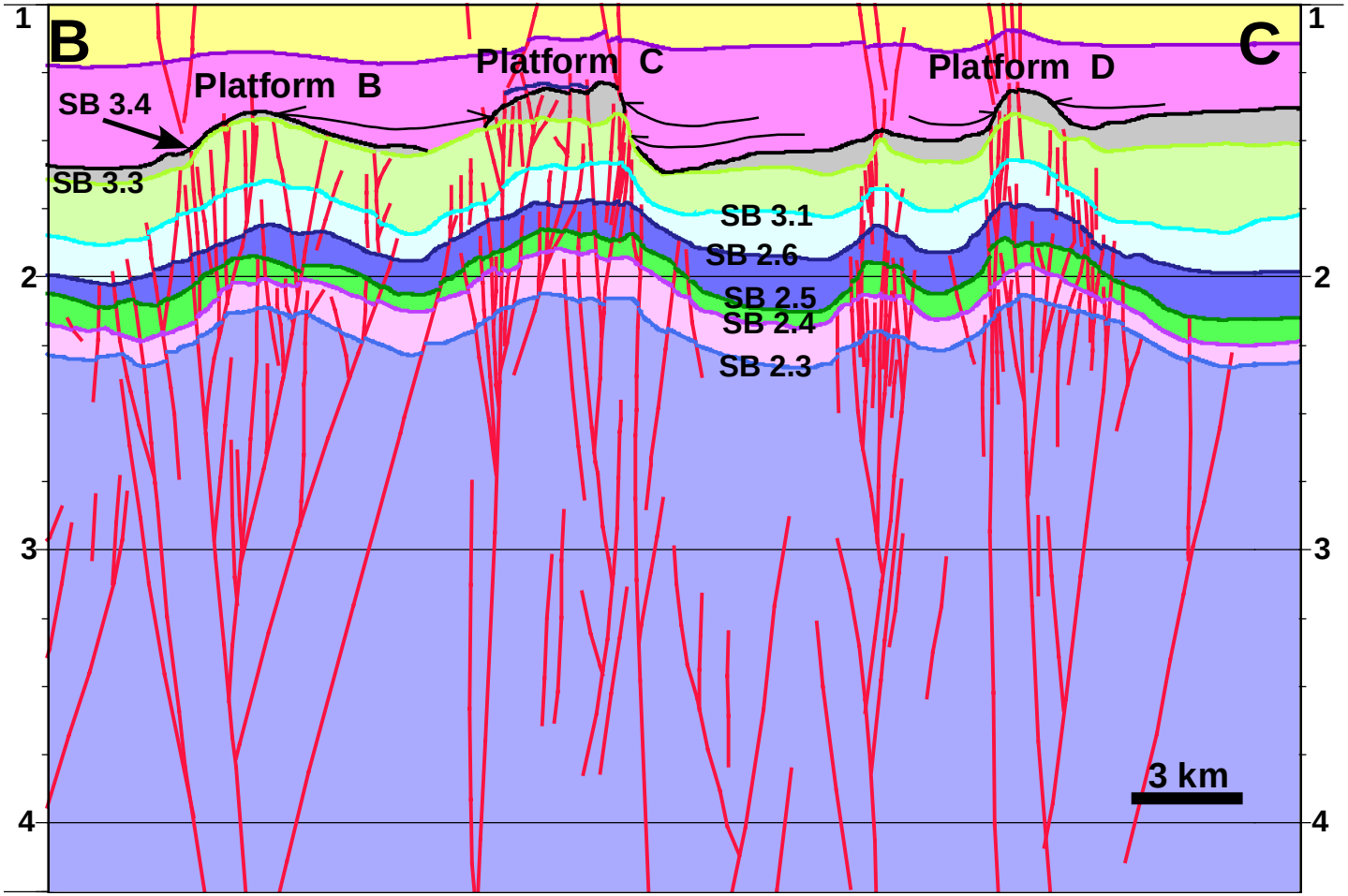

Figure 14. Interpretation from seismic profile B-C (see Figure 12 for line location). The figure shows platforms B, C and D. Siliciclastic sediments onlapping against carbonate platform flanks indicates that siliciclastics arrived to the platforms after drowning.

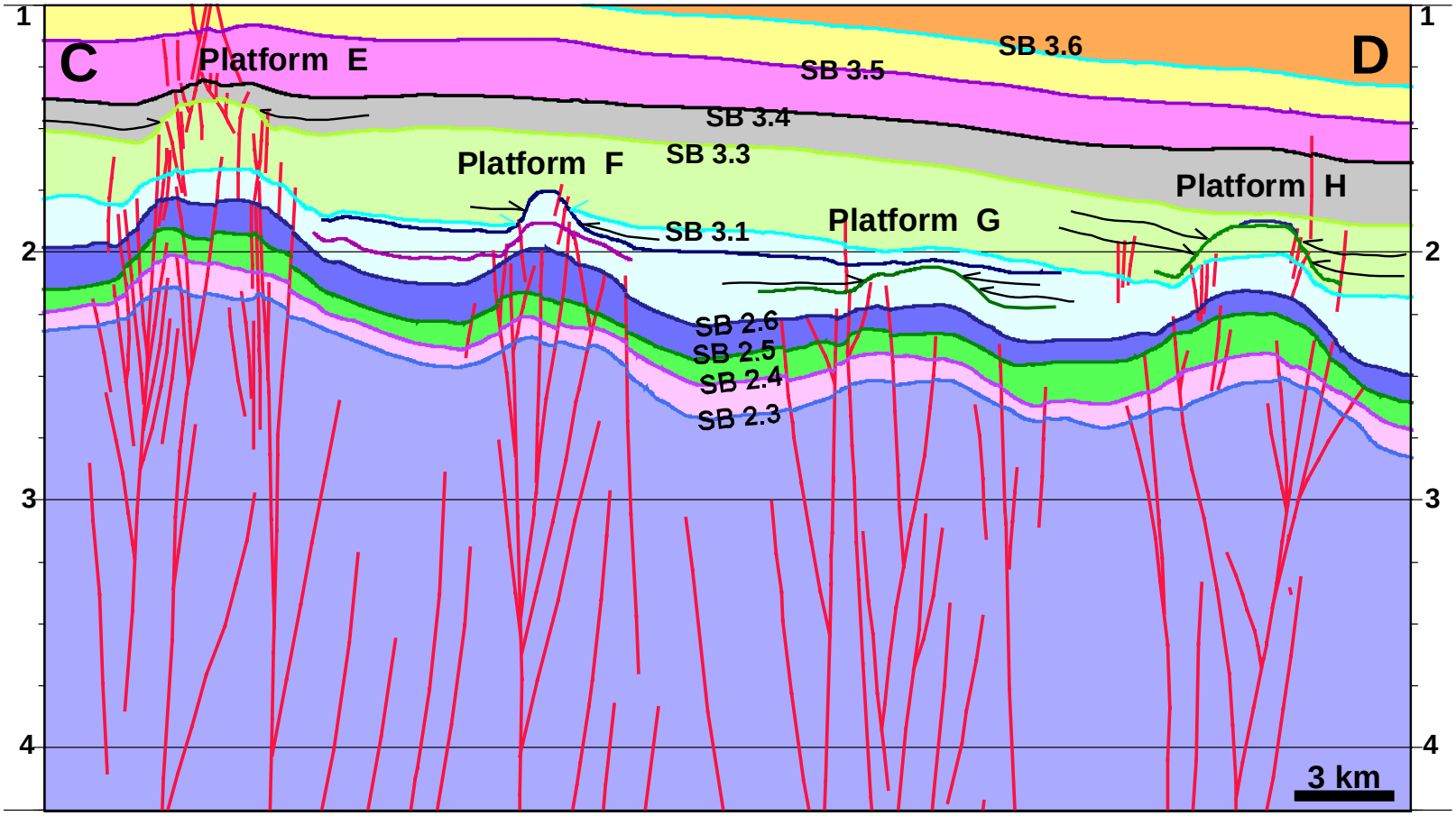

Figure 15. Interpretation from seismic profile C-D (see Figure 12 for line location). The figure shows platforms E, F, G and H. It is evident from reflector termination patterns within siliciclastic facies that the first platform of this segment of line to be drowned was Platform G, closely followed by Platform F, then Platform H, and finally Platform E.

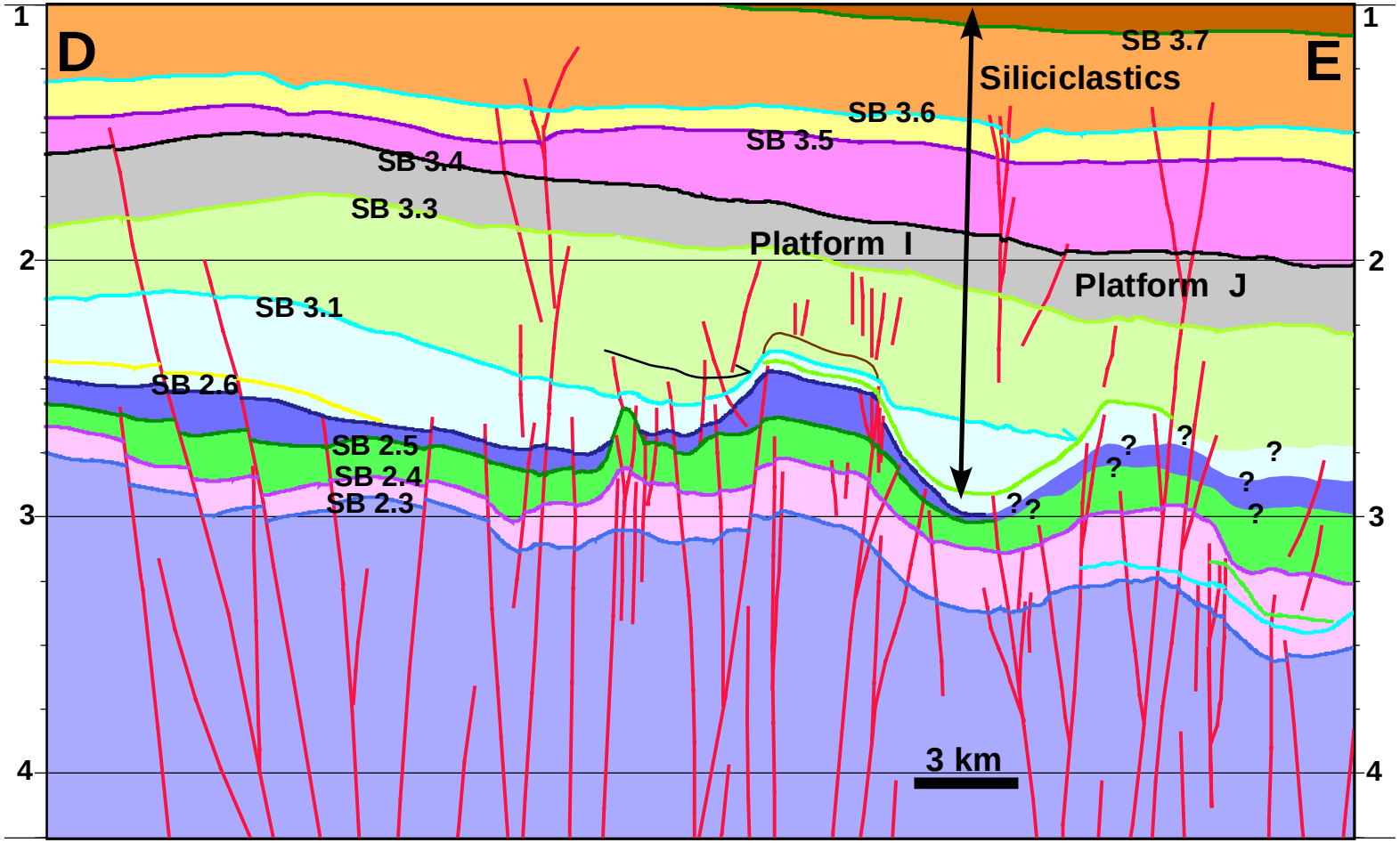

Figure 16. Interpretation from seismic profile D-E (see Figure 12 for line location). The figure shows platforms I, J and K. It is evident from the figure the flexural subsidence increasing towards the east.

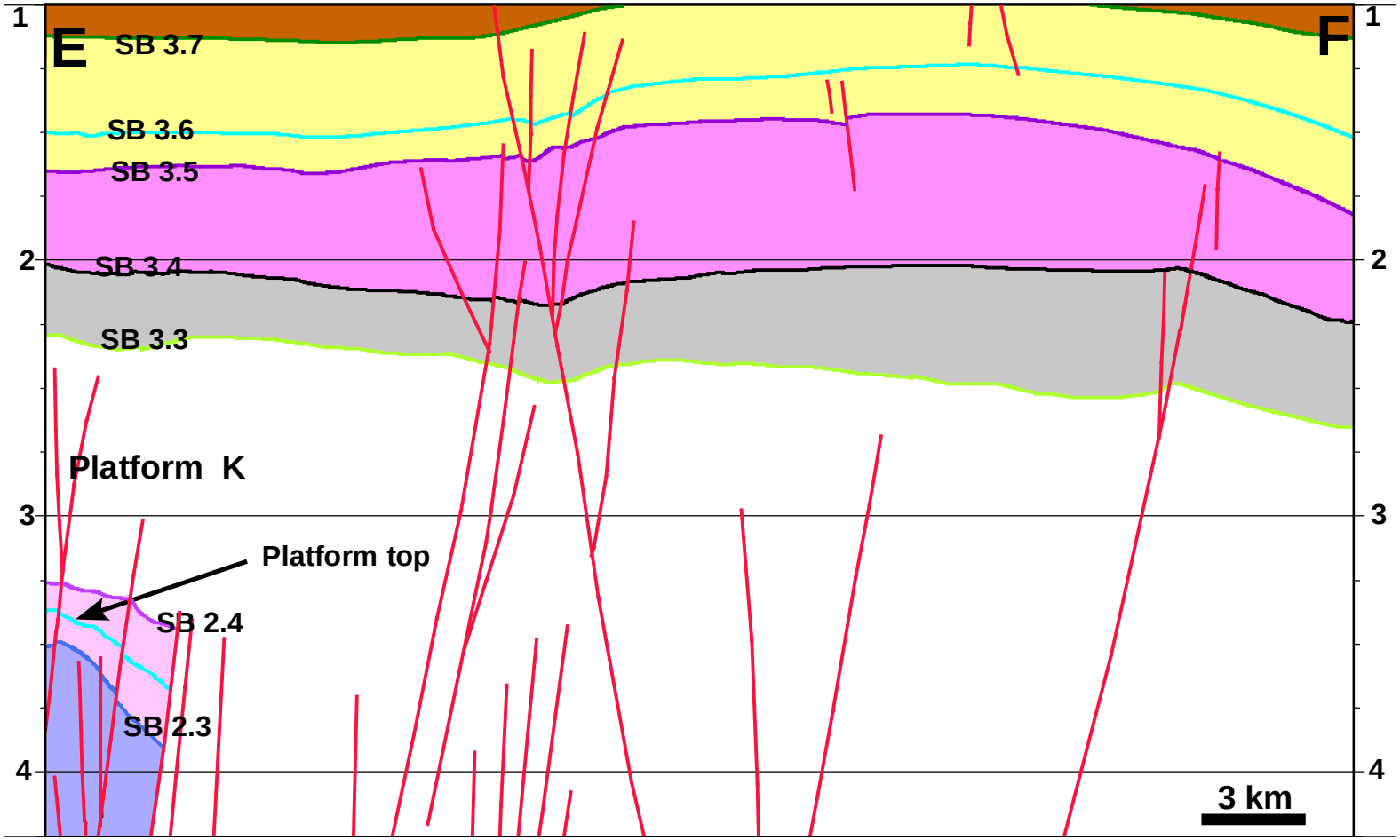

Figure 17. Interpretation from seismic profile E-F (see Figure 12 for line location). The figure shows Platform K, which was the first platform to be drowned in the area. The area to the east and below marker SB 3.3 was not interpreted because the resolution of the seismic data was very poor.

Table 2. Thicknesses (in meters) of the different third-order cycles across the carbonate platforms measured over the E-W seismic profile.

Plat.	Cycle 2.3	Cycle 2.4	Cycle 2.5	Cycle 2.6	Cycle 3.1	Cycle 3.3	TOTAL (m)
A	220	216	156	292	452	44	1380
B	212	194	196	330	488	56	1476
C	300	164	180	292	322	234	1492
D	224	160	264	332	308	212	1500
E	264	196	288	290	516	Terminated	1554
F	156	196	312	516	Terminated	Terminated	1180
G	218	172	246	246	Terminated	Terminated	882
H	240	316	216	248	304	Terminated	1324
I	404	160	464	156	108	Terminated	1292

Two-dimensional widths of carbonate platforms in the seismic lines were measured over the different third-order cycles (Table 3). Platform width is typically greater for the first two growth cycles (cycles 2.3 and 2.4) and decrease during subsequent growth cycles as most platforms backstepped. Widths range from 2.5 to 6.5 km and correlate with platform thickness (wider platforms associated with thicker platforms). Thus, wider platform are located in the western part of the seismic profile.

Table 3. Platforms widths (in kilometers) across the E-W seismic profile measured over the different third-order cycles.

Platform	Cycle 2.3	Cycle 2.4	Cycle 2.5	Cycle 2.6	Cycle 3.1	Cycle 3.3
A	6.5	6.5	6.5	6.5	4.9	4
B	2.5	2.8	3	3.2	3.6	2
C	3.2	3.2	3.2	3.5	4	3
D	2.4	2.5	2.5	2.5	2.7	1.6
E	3.6	3.6	3.6	3.6	3	Terminated
F	2.8	2.8	2.8	1.6	Terminated	Terminated
G	4	4	4	3.4	Terminated	Terminated
H	4.3	4.3	4	4	2.7	Terminated
I	3	3.5	3.5	3.5	3.3	Terminated

Carbonate platform slope angles were measured at the last Growth Stage of each platform (Figure 18). The horizontal distance “a” was measured in meters. The height of the slope “b” was measured in milliseconds, and then converted to depth (meters) using a velocity for siliciclastic sediments of approximately 4,000 m/s (Kearey and Brooks, 1991). The trigonometric function shown in Figure 18 was then applied to calculate slope angle in degrees. Results show that platforms have different slope inclinations on their flanks (Table 4). Platforms C, G and H have a steeper slope on their eastern flank than on their western flank. Platforms A, B, D and F have steeper slopes on their western flank. The remaining platforms (E and I) are more symmetrical, at least along this 2D section, showing approximately similar slopes on either flank. Although platform width and slope angle could only be measured on a single, 2D profile, important regional trends are apparent, as discussed below.

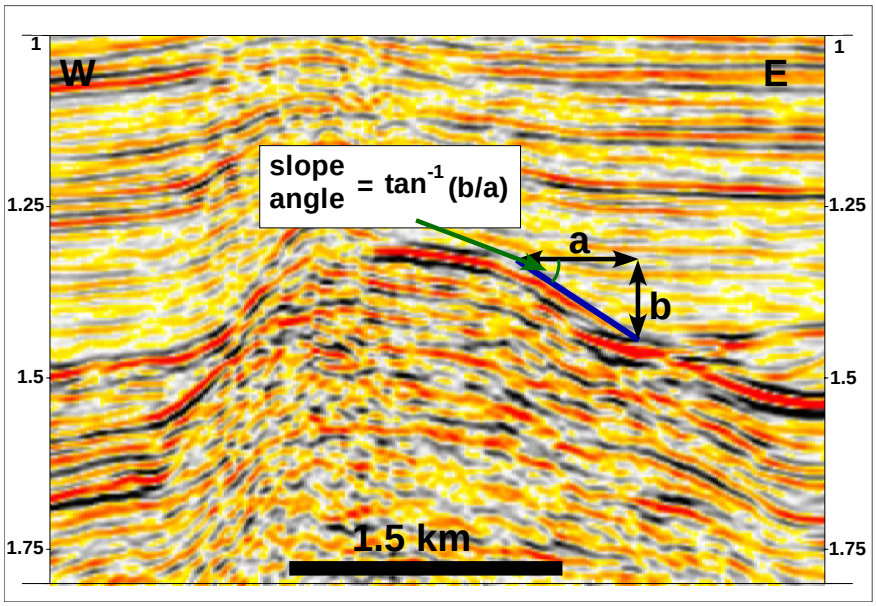

Figure 18. Procedure used to calculate slope angles on carbonate platforms.

Platform profiles are variable across the seismic section. Most platforms are flat-topped to mound-shaped isolated platforms. There is no apparent relationship between platform shape and total or interval thickness.

Growth Stages within each platform were identified by applying standard seismic stratigraphic concepts and principles, and carefully comparing similar growth patterns of platforms (cf. Zampetti et al., 2004). Mapable horizons followed those defined by Shell's terminology for Central Luconia shown on an interpreted seismic profile in Vahrenkamp et al. (2004). Each identified seismic unit defines a third-order (i.e., order of myr) depositional cycle. An exception is the seismic unit between markers SB 3.1 and SB 3.3, which represents two third-order cycles because sequence boundary SB 3.2 is not shown in the interpreted section of Vahrenkamp et al. (2004).

Table 4. Platform flank inclinations (in degrees) of the different carbonate platforms across the E-W seismic profile.

Platform	Western flank slope	Eastern flank slope
A	25º	5º
B	13º	7.8º
C	10º	20º
D	20º	10º
E	15.5º	12.5º
F	9º	5.5º
G	12º	24º
H	15º	25º
I	12º	16º

Carbonate deposition was generally coeval in most Luconia platforms and began with the deposition of the Cycle 2.3 (~16.5 Ma). The base of this cycle is seismically characterized by a high-amplitude reflector in most platforms. Five Growth Stages were identified above this high-amplitude reflector within carbonate platforms of the Luconia area.

Growth Stage 1

The first two seismic units (Cycles 2.3 and 2.4) comprise Growth Stage 1, and are characterized by aggradational stratal patterns in all platforms. Growth Stage 1 (GS1) is underlain by SB 2.3 at its base and SB 2.5 at its top. GS1 is 350 m to 450 m (175 to 225 ms) thick, with the exception of Platform I, where platform thickness exceeds 550 m (275 ms) (Table 5). GS 1 is characterized by chaotic and low-amplitude (locally semi-transparent) parallel to sub-parallel, gently dipping, inner platform reflectors. Platform margin seismic facies are characterized by low-amplitude reflectors with chaotic to nearly transparent internal seismic character.

Table 5. Thickness (in meters) of the different Growth Stages within Luconia carbonate platforms as measured on the E-W seismic profile.

Platform	GS1	GS2	GS3	GS4	GS5	TOTAL (m)
A	436	156	292	452	44	1380
B	406	196	330	488	56	1476
C	464	180	292	322	234	1492
D	384	264	332	308	212	1500
E	460	288	288	516	Terminated	1552
F	352	312	516	Terminated	Terminated	1180
G	388	246	246	Terminated	Terminated	880
H	556	216	248	304	Terminated	1324
I	564	464	156	108	Terminated	1292

Growth Stage 2

Growth Stage 2 (GS2) is bounded by markers SB 2.5 and SB 2.6. Platforms across the E-W seismic profile are 200 m to 300 m thick (100 to 150 ms), except for the three platforms located on the westernmost part of the seismic profile (platforms A, B and C), where the thicknesses corresponding to GS2 are below 200 m (100 ms).

Seismic facies within GS2 are similar to GS1, and are characterized by aggradational stratal geometries, with the exception of Platform H, which shows slight backstepping of its margins during the transition from GS1 to GS2.

Growth Stage 3

Growth Stage 3 (GS3), between markers SB 2.6 and SB 3.1 has variable stratal geometries in different platforms. Some platforms were terminated during this Growth Stage, whereas others kept growing. GS3 is ~300 m (150 ms) thick in most platforms, with the exception of Platforms F, G, H and I, where thickness exceeds 500 m (250 ms) in Platform F, and is below 248 m (124 ms) in Platforms G (246 m), H (248 m), and I (156 m). GS3 is characterized by low amplitude, semi-transparent, horizontal to gently dipping reflectors in inner platform facies, whereas platform margin facies are characterized by low-amplitude, convex upward to slightly chaotic reflectors.

Growth Stage 3 is largely aggradational in most platforms, with the exceptions of Platforms F and G, which show backstepping geometries, and Platform H, which shows aggradational to progradational geometries. At the transition from GS2 to GS3, platforms D, E and H show slight backstepping of the platform margins.

Growth Stage 4

Growth Stage 4 (GS4) lies between markers SB 3.1 and SB 3.3. As GS3, GS4 has different geometries in different platforms. GS4 is ~300 m (150 ms) thick in Platforms C, D and H, ~500 m (250 ms) thick in Platforms A, B and E, and ~100 m (50 ms) in Platform I. GS4 is characterized in most platforms by continuous and horizontal reflectors with an average magnitude of amplitude (stronger than in Growth Stages 1, 2 and 3).

Growth Stage 4 shows aggradational stratal geometries in Platforms A, B and I, whereas platforms C and D show aggradational to progradational stratal geometries. Platforms H and E show backstepping geometries (GS4 is the last Growth Stage in these platforms).

Growth Stage 5

Growth Stage 5 (GS5) is underlain by marker SB 3.3 and overlain by SB 3.4. GS5 is ~50 m (25 ms) thick in Platforms A and B, whereas is over 200 m (100 ms) thick in platforms C and D. GS5 is characterized by continuous reflectors with average-amplitude.

Growth Stage 5 shows backstepping stratal geometries in platform C and D, whereas in platforms A and B GS5 is represented by a thin carbonate layer blanketing platform tops.

N-S Trending Profile

The N-S trending seismic profile (Figure 19) is approximately 168 km long and intersects seven carbonate platforms located in tectonic highs. From north to south the carbonate platforms were labeled: platform L-R. There are also three carbonate pinnacles in basinal areas: two at both sides of platform N, and one northward of platform Q.

As in the E-W seismic profile, carbonate platform thicknesses were measured in two-way travel time (Table 6), and then converted to depth (Table 7). Results indicate that thicknesses range from 964 m (482 ms) in platform P to 1832 m (916 ms) in platform O. Platforms located to the northernmost part of the seismic profile tend to be thinner (they barely reach 1300 m of thickness) than platforms to the southern part, where most of them exceed the 1550 m of thickness (Figures 20 through 23).

Table 6. Thicknesses (in miliseconds) of the different third-order cycles across the carbonate platforms measured over the N-S seismic profile.

Plat.	Cycle 2.3	Cycle 2.4	Cycle 2.5	Cycle 2.6	Cycle 3.1	Cycle 3.3	TOTAL (ms)
L	193	79	109	68	79	109	637
M	124	206	126	82	56	76	670
N	266	204	206	140	Terminated	Terminated	816
O	130	114	146	420	106	Terminated	916
P	98	178	206	Terminated	Terminated	Terminated	482
Q	60	194	174	208	130	45	811
R	116	82	252	232	Terminated	Terminated	682

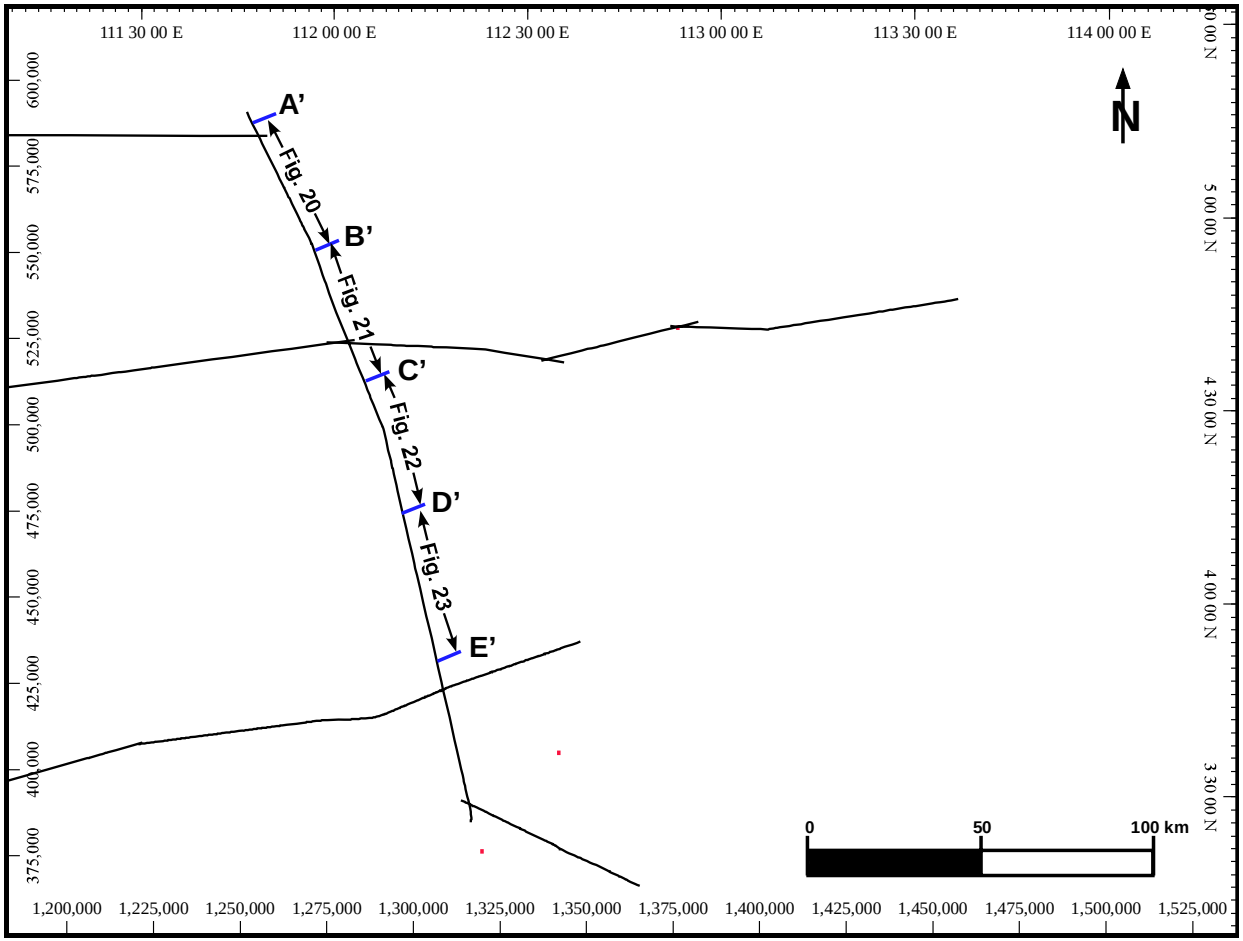

Figure 19. Location of N-S seismic profiles used for this study (from the SEAS 95 “Supertie” Seismic Survey).

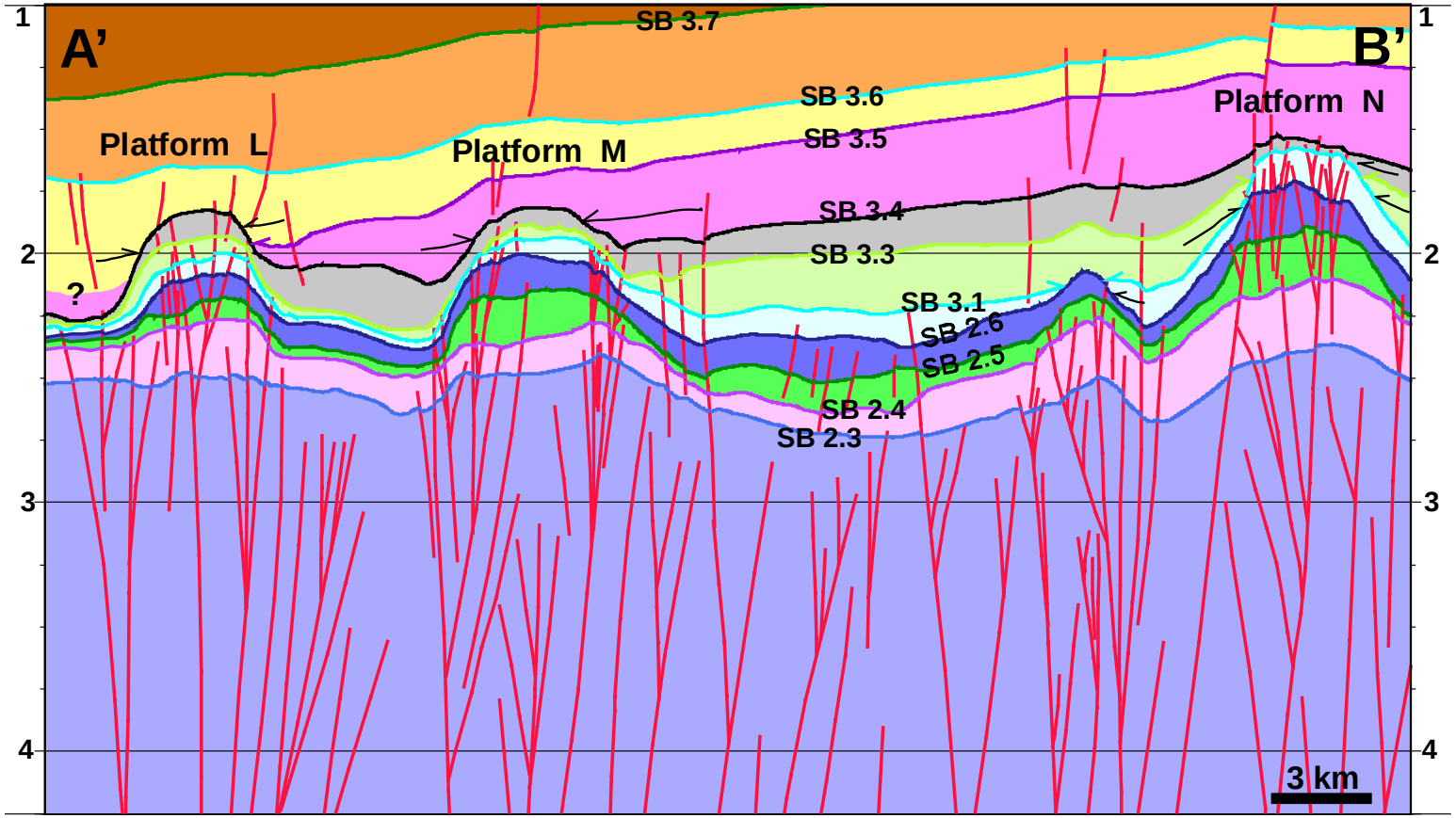

Figure 20. Interpretation from seismic profile A’-B’ (see Figure 19 for line location). The figure shows platforms L, M and N. Platforms L and M are the last platforms to be covered by siliciclastic sediments in the area.

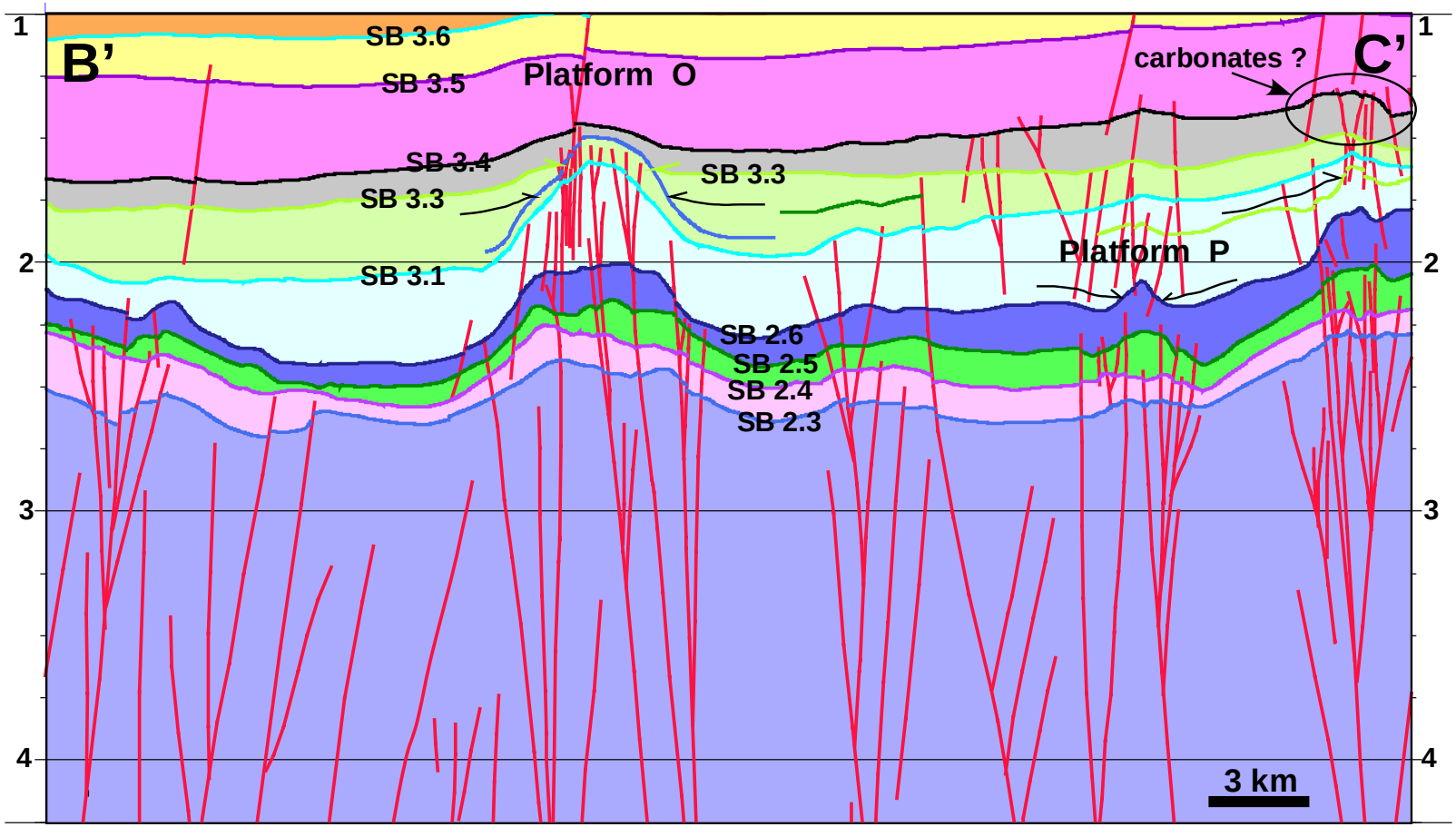

Figure 21. Interpretation from seismic profile B’-C’ (see Figure 19 for line location). The figure shows platforms O and P.

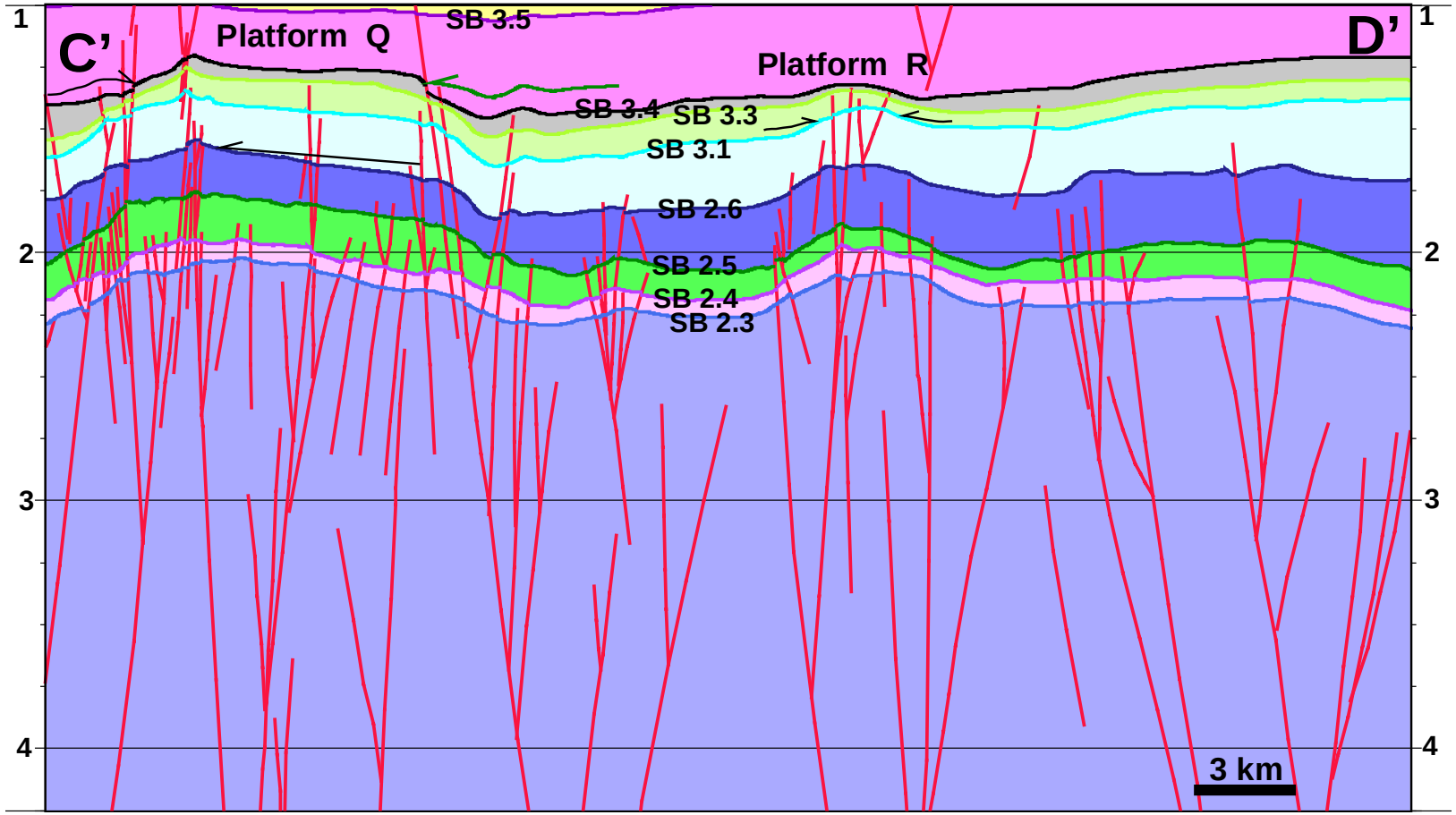

Figure 22. Interpretation from seismic profile C'-D' (see Figure 19 for line location). The figure shows platforms Q and R. The development of wedge-shaped stratigraphy in Platform Q during Growth Stage 3 is caused by differential subsidence along the platform-bounding faults.

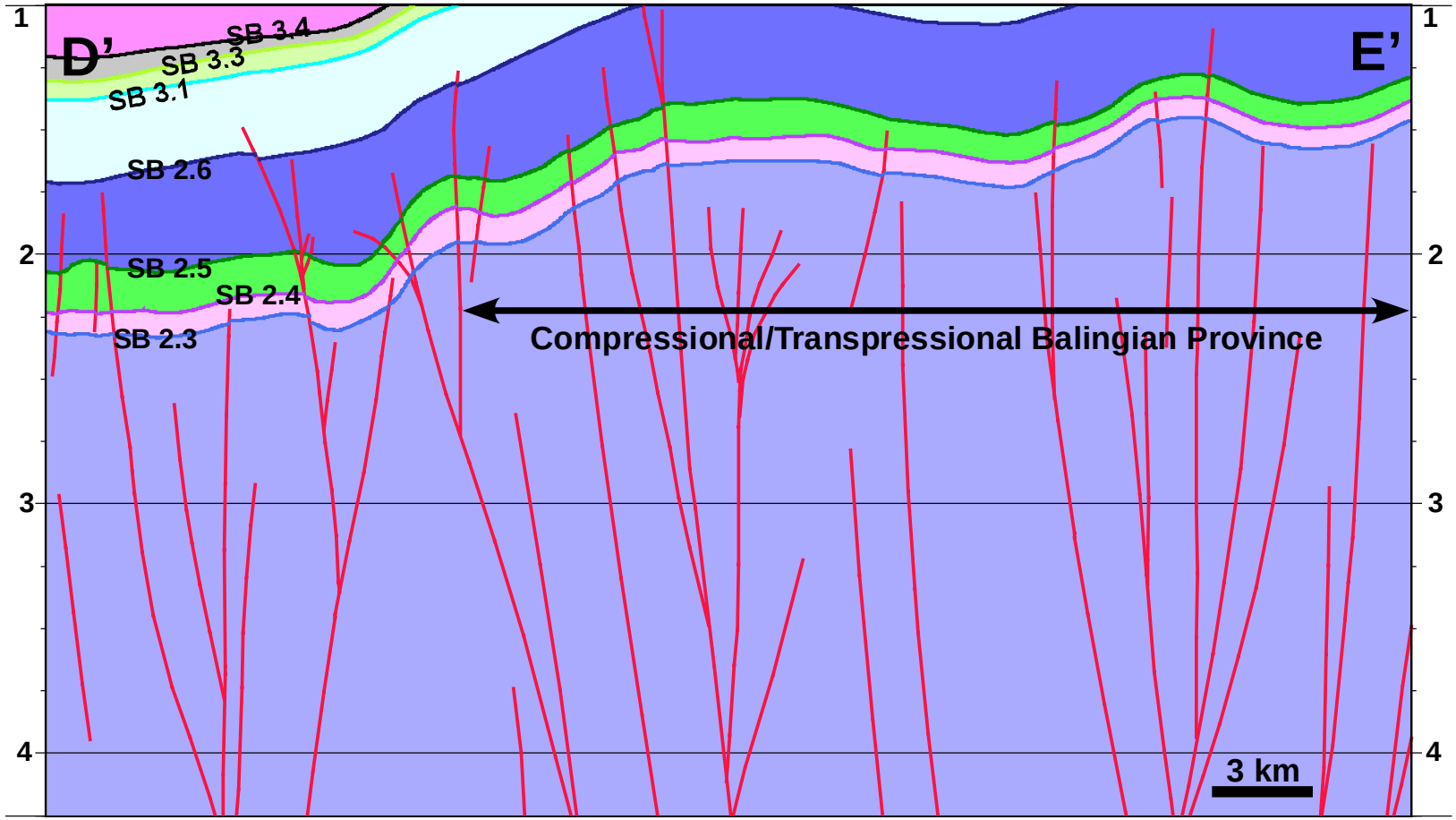

Figure 23. Interpretation from seismic profile D’-E’ (see Figure 19 for line location). The figure shows the southernmost part of Central Luconia Province where is evident the transition into the Balingian Province to the south.

Two-dimensional widths of the carbonate platforms in the seismic profiles were measured over the different third-order cycles (Table 8). Results indicate that carbonate platforms have an average length between 2.5 km to 4 km, with the exception of Platform Q, which has ~7.1-8.2 km of width, and Platform P which has ~2.3 km of width. Pinnacles have an average width of approximately 1.8 km. Unlike the E-W seismic profile, there is not a visible trend between platform width and location along the N-S seismic profile.

Table 7. Thicknesses (in meters) of the different third-order cycles across the carbonate platforms measured over the N-S seismic profile.

Plat.	Cycle 2.3	Cycle 2.4	Cycle 2.5	Cycle 2.6	Cycle 3.1	Cycle 3.3	TOTAL (m)
L	386	158	218	136	158	218	1274
M	248	412	252	164	112	152	1340
N	532	408	412	280	Terminated	Terminated	1632
O	260	228	292	840	212	Terminated	1832
P	196	356	412	Terminated	Terminated	Terminated	964
Q	120	388	348	416	260	90	1622
R	232	164	504	464	Terminated	Terminated	1364

Table 8. Platforms widths (in kilometers) across the N-S seismic profile measured over the different third-order cycles.

Plat.	Cycle 2.3	Cycle 2.4	Cycle2.5	Cycle 2.6	Cycle 3.1	Cycle 3.3
L	2.5	2.5	2.8	2.9	3	2.7
M	3.7	3.7	3.8	3.9	2.7	2.5
N	3.5	3.5	3	2.8	Terminated	Terminated
O	4	4	4	3	1.7	Terminated
P	2.3	2.3	1.7	Terminated	Terminated	Terminated
Q	8.2	8.2	8	7.8	7.7	7.1
R	2.5	2.5	2.5	1.9	Terminated	Terminated

Carbonate platform slope angles were measured using the same procedure as in the E-W seismic profile (Figure 18). Platforms along the N-S seismic profile are asymmetric (Table 9), with northern flanks steeper than southern flanks.

Table 9. Platform flank inclinations (in degrees) of the different carbonate platforms across the N-S seismic profile.

Platform	Northern flank slope	Southern flank slope
L	32º	24º
M	22º	13º
N	24º	20º
O	25º	19º
P	13º	15º
Q	15º	8º
R	11º	5º

Platform profiles are also variable across the seismic lines. In the N-S seismic line there is just one platform that shows a flat-topped profile (Platform Q). The rest of the platforms have more mounded profiles.

Markers SB 2.3 to SB 3.8 were traced from the E-W seismic profile to the N-S seismic line, passing through carbonate platforms and basinal inter-platform regions. As in the E-W seismic profile, five Growth Stages were identified during the interpretation, named from bottom to top as Growth Stage 1 to 5.

Growth Stage 1

Growth Stage 1 (GS1) is underlain by marker SB 2.3 (characterized by a high-amplitude reflector) at its base and SB 2.5 at its top. GS1 is ~400 m (200 ms) to ~650 m (375 ms) thick in all platforms, excepting Platform N, which is 940 m (470 ms) thick

(Table 10). GS1 is characterized by low-amplitude (locally semi-transparent) parallel to subparallel inner platform reflectors, whereas platform margin seismic facies are characterized by chaotic to nearly transparent internal seismic facies. All platforms in the N-S seismic profile show aggradational stratal geometries in GS1.

Table 10. Thickness (in meters) of the different Growth Stages within Luconia carbonate platforms as measured on the N-S seismic profile.

Platform	GS1	GS2	GS3	GS4	GS5	TOTAL (m)
L	544	218	136	158	218	1274
M	660	252	164	112	152	1340
N	940	412	280	Terminated	Terminated	1632
O	488	292	840	212	Terminated	1832
P	552	412	Terminated	Terminated	Terminated	964
Q	508	348	416	260	90	1622
R	396	504	464	Terminated	Terminated	1364

Growth Stage 2

Growth Stage 2 (GS2) is bounded by markers SB 2.5 and SB 2.6. Platforms in the N-S seismic profile are ~350 m (175 ms) to 550 m (275 ms) thick in all platforms, excepting platforms L and M, where the thickness of GS2 does not exceed 260 m (130 ms).

Growth Stage 2 is characterized by low-amplitude (locally semi-transparent), gently dipping reflectors, similar to Growth Stage 1. GS2 show three different stratal geometries: backstepping in Platform P, aggradational to progradational in platforms L and M, and aggradational in platforms N, O, Q and R. Although platform N shows

mostly aggradational stratal geometries during GS2, there is also an evident backstepping of the platform margins from GS 1 to GS2.

Growth Stage 3

Growth Stage 3 (GS3), between markers SB 2.6 and SB 3.1, is characterized by low-amplitude, parallel to gently dipping reflectors in inner platforms facies, and low-amplitude and chaotic to semi-transparent reflectors in margin platform seismic facies. Growth Stage 3 has variable stratal geometries in different platforms because during GS3 some platforms were terminated (Platforms R and N), while other showed aggradational (Platform Q), aggradational to progradational (Platforms L and M), and aggradational to backstepping (Platform O) stratal geometries.

Growth Stage 3 is 160 m (80 ms) thick in the northernmost platforms (Platforms L and M), ~280 m (140 ms) thick in platform N, and is above 400 m (200 ms) thick in the southernmost platforms (Platforms Q and R). Platform O has an abnormal thickness of 840 m (410 ms) during GS3.

Growth Stage 4

Growth Stage 4 (GS4) lies between markers SB 3.1 and SB 3.3. Growth Stage 4 is characterized by parallel to subparallel, continuous reflectors in inner platform facies (with higher amplitudes than in previous Growth Stages), and discontinuous and chaotic low-amplitude reflectors in margin platform seismic facies. Growth Stage 4 is ~200 m (100 ms) to 250 m (125 ms) thick in platforms O and Q, and approximately 110 m (55 ms) to 160 m (80 ms) thick in platforms L and M.

Platform O shows aggradational to backstepping stratal geometries in GS4, whereas platform Q shows aggradational stratal geometries in GS4. Platforms to the northernmost part of the N-S seismic profile (Platforms L and M) show aggradational to progradational stratal geometries.

Growth Stage 5

Growth Stage 5 (GS5) is underlain by marker SB 3.3 and overlain by marker SB 3.4. Growth Stage 5 shows thicknesses just in three platforms (Platforms L, M and Q). Platforms L and M are ~150 m (75 ms) to ~220 m (110 ms) thick in GS5, and they show aggradational to backstepping stratal geometries. Platform Q is just 84 m (42 ms) thick in GS5. Although the thickness of GS5 in Platform Q is very thin (which makes hard to decipher the stratal geometry), it can be identified that the stratal geometry in GS5 is aggradational.

Growth Stage 5 is characterized by low-amplitude (locally semi-transparent), parallel to subparallel, gently dipping reflectors in inner platform seismic facies.

Interpretation

From both regional 2-D seismic profiles is evident that carbonate accumulation was generally coeval in all platforms of Luconia carbonates, and was initiated during the deposition of the third-order cycle 2.3, which began at ~16.5 Ma. The base of the carbonate platforms is characterized by a high amplitude reflector represented by marker SB 2.3 (Figure 24). The analysis of carbonate growth evolution results in the

identification of five Growth Stages of carbonate accumulation across the study area; these are, in ascending order, Growth Stages 1 to 5.

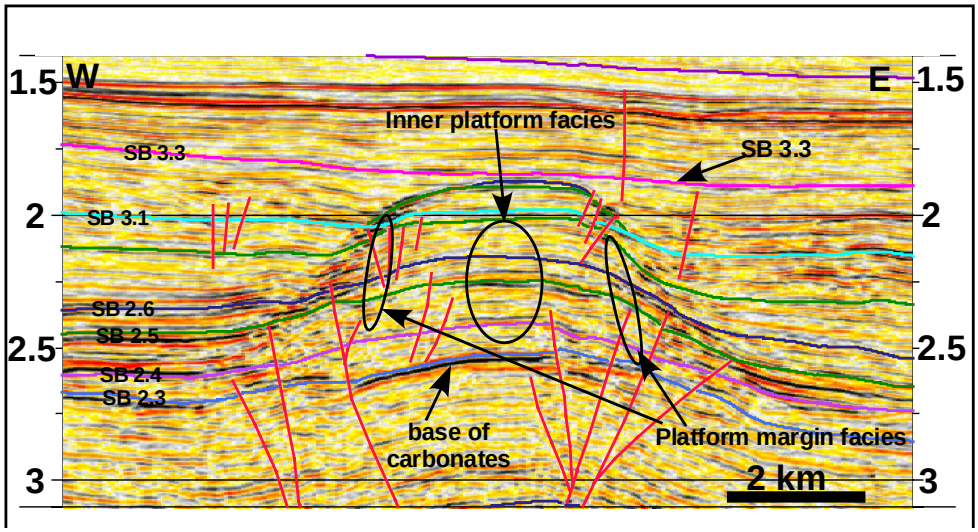

Figure 24. Platform H showing major faults with small displacements and minor faults upwards with even smaller displacements. The base of carbonates is characterized by a high-amplitude reflector.

All platforms in GS1 and GS2 show aggradational stratal geometries. According to the sea-level curve of Haq et al. (1988) (Figure 4), Growth Stages 1 and 2 were deposited during a second-order sea-level highstand period, which along with the long-term subsidence produced aggradational stratal geometries. Platforms I and J are the only platforms that do not show aggradational stratal geometries during GS1 because platform-bounding faults did not generate a steep bathymetric gradient, and thus carbonates facies were slightly prograded during GS1.

Stratal geometries during GS3, and GS4 are highly variable because during these Growth Stages some platforms backstepped and were terminated while others kept

growing. Those platforms that were terminated could not keep pace with the sea-level rise and long-term tectonic subsidence, and ultimately sunk beneath the photic zone. Platforms that kept growing show aggradational and aggradational to progradational stratal geometries. All platforms show backstepping stratal geometries during their last Growth Stage. The only platforms that do not show backstepping stratal geometries during their last Growth Stage are platforms I and J, possibly because they suffered an environmental deterioration due to siliciclastic influx from mainland Borneo, and also had a rapid increment of the flexural subsidence affecting that part of Luconia carbonates area.

Differences in stratal geometries in different platforms were reflect three main factors: (1) third-order sea-level fluctuations, (2) long-term tectonic subsidence, and (3) possible flexural subsidence affecting the easternmost part of the study area.

Carbonate accumulation rate data (Table 11) indicate that the accumulation rate of GS2 was slightly greater than the accumulation rate of GS1, and that average accumulation rates during both were faster than subsequent Growth Stages. Comparison to the sea-level chart of Haq et al., (1988) (Figure 4) shows that GS1 and GS2 were deposited during a second-order sea-level highstand period that possibly produced the thicknesses showed by GS1 and GS2 (Tables 5 and 10), the faster accumulation rates displayed by GS1 and GS2 (Table 11), and resultant stratal geometries during GS1 and GS2. Slower accumulation rates during Growth Stages 3 and 4 are possibly associated with sea-level fall in the second-order sea-level curve (Haq et al., 1988) between markers SB 2.6 and SB 3.3 (Figure 4).

Regionally, platforms in Central Luconia Province show aggradational stratal geometries during GS1, except toward the east, where fault activity during that time allowed platforms I and J to develop aggradational to progradational stratal geometries. Subsequently, during GS2 and GS3, platforms I and J showed aggradational stratal geometries due to the progressive development of flexural subsidence in the easternmost part of the study area. This flexural subsidence in the E-W seismic profile is possibly related to the load of siliciclastic sediments deposited in the easternmost part of the study area, and propagated westward and northwestward (based on clinoform dip directions) as the siliciclastic wedge prograded and became thicker. This migrating wave of flexural subsidence may have caused the termination of some platforms during GS3 and GS4.

Table 11. Long-term accumulation rates (in m/my) shown by each Growth Stage in Central Luconia platforms.

Platform	Stage 1	Stage 2	Stage 3	Stage 4	Stage 5	Average
A	161	120	146	108	55	125
B	150	151	165	116	70	134
C	172	138	146	77	293	136
D	142	203	166	73	265	144
E	170	222	144	123	Terminated	152
F	130	240	258	Terminated	Terminated	262
G	144	189	123	Terminated	Terminated	215
H	206	166	124	72	Terminated	210
I	264	243	78	26	Terminated	199
L	201	168	68	38	273	116
M	244	194	82	27	190	122
N	348	317	140	Terminated	Terminated	272
O	181	225	420	50	Terminated	269
P	204	317	Terminated	Terminated	Terminated	241
Q	188	268	208	62	113	147
R	147	388	232	Terminated	Terminated	261

After GS1, subsidence is inferred to have been greater in the southern and central part of the N-S seismic profile, where platforms N, O, P, Q and R show aggradational and backstepping stratal geometries during Growth Stages 2, 3, 4 and 5. In platforms L and M subsidence decreased after GS1, and continued to be slower than in central and southern parts of the area until the termination of both platforms during GS5. This decrease in the subsidence is responsible for the aggradational to progradational stratal geometries displayed by these two platforms.

Figure 25 depicts the history of platform termination along the available seismic lines. The first platform terminated was Platform K at the easternmost part of the Central Luconia area, east of Platform J. Platform K was terminated by siliciclastic influx from mainland Borneo, which created a combined affect of flexural subsidence and environmental deterioration. There is no evidence of a drowning unconformity because the quality of the data is not good in that area, but mapping of sequence boundaries from adjacent platforms suggests that Platform K was terminated at ~16 Ma.

A carbonate pinnacle on the basinal area close to Platform I was the next build-up terminated (~13.8 Ma). The next platform terminated was Platform P at ~12.5 Ma, which may have been related to rapid tectonic subsidence as suggested by the intense faulting around the platforms margins. Shortly after (at ~12.4 Ma) carbonate pinnacles in basinal areas, first southward, and then northward of platform N were terminated.

The pinnacle at the northern basinal area of Platform Q was terminated next (at about 11.5 Ma). It was closely followed by the termination of platforms J (~11.4 Ma), G

(~11.3 Ma), F (~11.0 Ma), and platforms R and N at approximately the same time (~10.5 Ma).

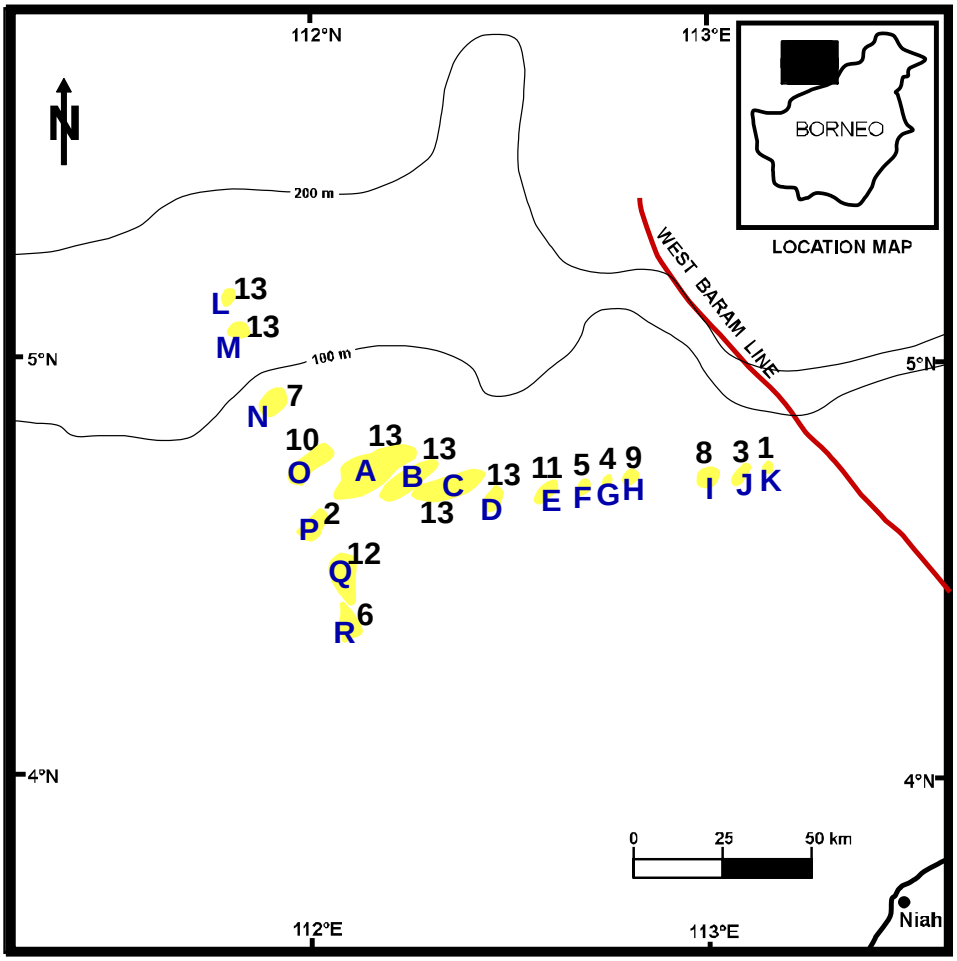

Figure 25. Carbonate platforms intersected by the seismic data in Central Luconia area. Numbers next to each platform indicate the order in which they were terminated, with # 1 being the first platform terminated and so on.

Platform I was terminated at ~10.0 Ma. Then were terminated platforms H (~8.2 Ma), O (~7.8 Ma), E (~6.3 Ma), and the small pinnacle in the basinal area westward of Platform D (~6.3 Ma). The final terminations, which occurred almost

simultaneously, affected platforms Q, D, C, B, A, L and M (~5.5 Ma). Cycle 3.3 was the last episode of carbonate accumulation in the study area, and it coincides with a high-amplitude and rapid sea-level rise, which prevented start-up of the carbonate factories across the study area. The low-amplitude character of the reflectors (representing deep-water sediments) overlying the sequence boundary SB 3.4 supports this interpretation.

Most of the termination events are preceded by backstepping stratal patterns, except platforms I, J and K, which show aggradational stratal geometries during their last Growth Stages, and platforms A, B and Q which also show aggradational stratal geometries during their last Growth Stages, but with very thin carbonate accumulations. Terminal pinnacle reefs prior to termination were seen in three platforms (C, D and F).

Most platform drowning sequences are defined by a high-amplitude/low-frequency reflector (Figure 26) enveloping platform tops, because the frequency content of the seismic data does not allow resolution of these typically thin sequences. These high-amplitude reflectors likely represent a shale cap or deep water limestone facies.

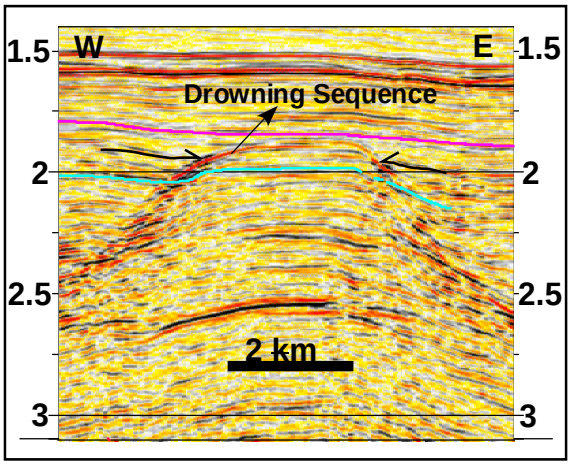

Figure 26. Drowning Sequence in Platform H.

The order of platforms termination (Figure 25) indicates that the first platforms terminated were closer to siliciclastic supply and to flexural subsidence in the eastern part of the study area (Platforms J and K), and those small platforms affected by a high degree of tectonic subsidence (Platforms P, G and F). Larger platforms that were subsequently drowned were affected by high subsidence and intense faulting (Platforms R, N and O), and by the increased flexural subsidence possibly caused by northwestward progradation of siliciclastic sediments (Platforms I, H and G). Finally the largest platform (Platform Q) was terminated due to increased tectonic subsidence and siliciclastic influx, and then almost simultaneously were terminated platforms D, C, B and A (due to increased tectonic and flexural subsidence coupled to a rapid sea-level rise), and platforms L and M (due to increased tectonic subsidence coupled to a rapid sea-level rise).

Third-order sea-level falls at the end of cycles 2.3 through 3.3 suggest a subaerial exposure of the platforms during these lowstand periods, but the data available only supports subaerial exposures for a few Growth Stages in a small group of platforms (platforms Q, N, E, D, and C). There is no evidence in the seismic data of karst features pre-dating carbonate platform terminations (Figure 27).

The N-S and E-W seismic lines are characterized by high dip normal and strike-slip faults that branch upward and formed flower structures around the area. Most of the elevated regions where carbonate platforms are seated were produced by strike-slip deformation and by some normal faults. The southernmost part of the N-S seismic profile (Figure 23) is characterized by compressive/transpressive structures that include

reverse and branching upward faults, and the formation of anticline produced by the deformation. This area belongs to the Balingian Geological province and does not show carbonate accumulation.

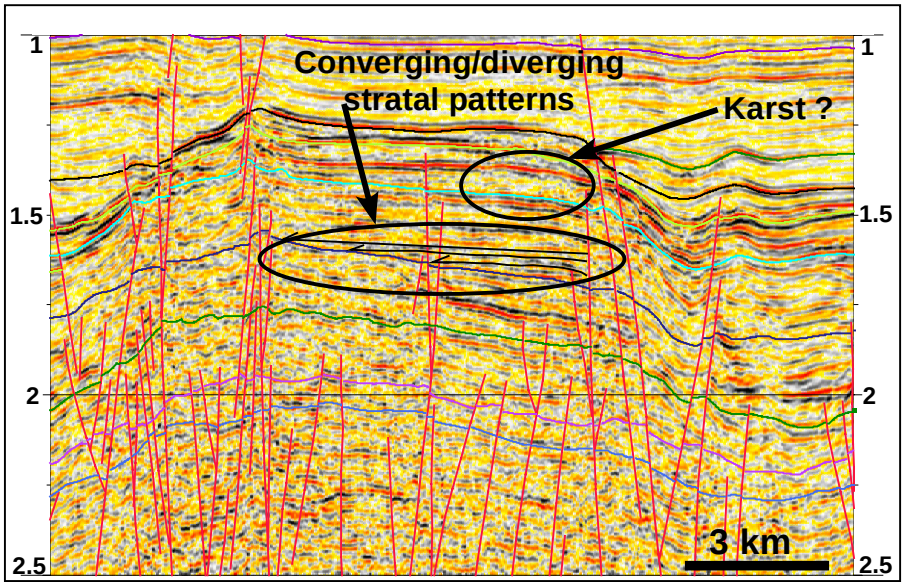

Figure 27. Karst features and converging/diverging stratal patterns in Platform Q.

Tectonic activity of strike-slip faults had an important role in the development of carbonate platforms in the Central Luconia Province because it created the structural highs where carbonate platforms began to accumulate, and also produced steep bathymetric gradients across the platform-bounding fault zones that prevented progradation of platform margins (excepting platforms I and J). Although in the seismic data strike-slip faults propagated upward through platform stratigraphy, they did not have a strong influence in the deposition of Growth Stages younger than GS2. Most of the faults in the E-W and N-S seismic profiles that propagated through carbonate facies

were smaller faults and did not influence overall stratal geometries. For instance, platform H (Figure 24) shows that faults have small displacement. Faulting that affected Growth Stages younger than GS2 is represented by smaller faults related to synsedimentary processes with even smaller displacement than the major strike-slip faults.

Platform Q shows a higher activity of platform-bounding faults in the southern flank than in the northern flank (Figure 27), which tilted the platform during Growth Stage 3 and developed converging/diverging stratal geometries. During GS3 the movement of bounding faults in platform Q was progressively leveled and by the end of GS3 the platform did not show any sign of tilting.

2-D seismic data available (Figures 14 through 23) indicates that thicker and wider platforms were developed on the southwesternmost part of the Central Luconia Province. These platforms show mostly aggradational internal strata, and in some later stages aggradational to backstepping stratal geometries. This trend in the size of the platforms could be related to the increase of the tectonic subsidence in the southern and central parts of the N-S seismic profile, and in the western region of the E-W seismic profile.

Most of the platforms in the E-W seismic profile do not show a consistent windward-leeward asymmetry during carbonate accumulation (~5.5-16.5 Ma), suggesting that winds were consistently variable during platforms deposition. However, there are a few platforms (Platforms H, D, C and A) that display an apparent windward-leeward sediment transport. For instance, platforms H and C show an apparent east-to-

west sediment transport, whereas platforms A and D show an apparent west-to-east sediment transport. In this case, where different platforms show different windward-to-leeward sediment transport directions, is hard to decipher the influence of the East Asian Monsoonal winds on platform architecture, mostly because the wind directions were almost perpendicular to the seismic profile.

All platforms in the N-S seismic profile have a higher angle of inclination on their northern flanks than in their southern flanks (Table 9), suggesting a consistent windward-leeward asymmetry (north-to-south sediment transport direction) during carbonate accumulation. This pattern follows the pattern of East Asian Monsoonal winds during that time (Vahrenkamp et al., 2004), where northwesterly winter winds had a major effect on carbonate accumulation than the weaker southwesterly summer winds (Figure 28). Thus, carbonates platforms provide a good record of the evolution of East Asian Monsoon winds.

Figure 28. Middle Miocene East Asian Monsoon winds direction during winter across Central Luconia Province (L) (after Vahrenkamp et al., 2004).

CHAPTER V

DISCUSSIONS

Carbonate deposition in the Central Luconia Province was initiated generally at the same time, coeval with the third-order sea-level cycle 2.3 (~16.5 Ma). Carbonate platforms nucleated on topographic highs produced mainly by strike-slip, and to a lesser extent, extensional deformation during Oligocene time.

In the study area, carbonate pinnacles have average 2-D widths of 2,000 to 3,000 m and were terminated at different times due to differential subsidence. Although is not common in the geologic record, these pinnacles were nucleated over topographic highs produced by faults and not by accretion due to local opportunism of the fauna.

The main factor controlling the distribution of stratal geometries within the carbonate platforms across the Central Luconia Province was the sea-level fluctuation, which was modified primarily by subsidence. In the study area, subsidence was due to long-term processes and was also produced by siliciclastic influx from mainland Borneo, which created a combined effect of flexural subsidence and environmental deterioration that did not provide favorable conditions for carbonate growth (decreased carbonate accumulation rates).

Thicker carbonate sequences and faster rates of carbonate accumulation shown by platforms during Growth Stages 1 and 2 correlated with a period of sea-level highstand on the second-order sea-level curve of Haq et al. (1988) during most of Middle Miocene time, supporting the fact that growth potential of platforms commonly

increases during a rise of sea-level (Kendall and Schlager, 1981). Subsequent Growth Stages 3 and 4 showed smaller accumulation rates and thicknesses, correlating with a long-term fall in the third-order sea-level change curve (Figure 4).

Platforms in the N-S seismic profile recorded the predominance of the northwesterly winter East Asian Monsoon winds over the weaker summer winds, which was reflected as a windward-leeward asymmetry in the platforms, having steeper slope on the windward flanks (northern side) than on the leeward flanks (southern side). Therefore, in general, existent intraplatform prograding sequences were directed toward the south. Conversely, the E-W seismic profile did not show any strong indication of a prevailing wind direction probably because seismic lines were almost perpendicular to the wind direction. As a matter of fact, two groups of platforms at the western extreme of the E-W seismic profile showed opposite windward-leeward asymmetries.

The load of prograding siliciclastic sediments located in the eastern part of the Luconia Province progressively affected platforms from east-to-west (augmenting subsidence through time toward the west) and produced an environmental deterioration (Erlich et al., 1993) in platforms closer to the eastern part of the study area. This thick load of sediments appears to be from the Baram Delta, from which siliciclastic sediments were dumped by rivers from mainland Borneo onto offshore areas to the north beginning in Middle Miocene time. Siliciclastic sediments subsequently prograded northward and northwestward during Middle and Late Miocene time.

Northward prograding siliciclastic sediments from mainland Borneo, specifically from the Rajang Flysch Belt, were dumped into Sarawak Basin and affected the

carbonate platforms in the southern part of the study area. According to Vahrenkamp et al. (2004), this siliciclastic influx was responsible for termination of platforms in the southern part of the Central Luconia Province. These prograding siliciclastic packages (which can be seen in Figures 22 and 23) produced an environmental deterioration in the area, enhancing the chances of termination.

Tectonic subsidence is an important factor that increased the accommodation space available for carbonates. Subsidence progressively decreases from east to west until approximately the location of platform C. Conversely, it is high in the central and southern part of the study area, and could be associated to the active tectonicism in northern Borneo during Miocene time.

Distribution of porosity and permeability is closely related to relative sea-level changes and sediment fabric (Sun and Esteban, 1994). Generally, good reservoir properties are related to dissolution by meteoric water when sea-level fall exposes platform tops. Episodes of subaerial exposure seem to be recorded in platform interior facies of some Central Luconia carbonate platforms (Figure 27), but there is no relationship between platform location and the presence of karst features. Other workers (Vahrenkamp, 1998; Ali, 1994) found diagenetic cycles associated with subaerial exposure during lowstand episodes in the Central Luconia Province, which are more intense towards the northern part of the area. However, with the 2-D seismic data available, which are basically one cross-section per platform, it is not possible to characterize the presence of subaerial exposure surfaces in the platforms of Central

Luconia Province, or to confirm this tendency in the reservoir properties across the study area.

Calculated accumulation rate data (Table 11) indicate that accumulation rates decrease as platform duration increases. According to Schlager et al. (1998) and Schlager (1999), sedimentation rates change proportionally to the inverse of the square root of time, which is corroborated by plotting carbonate accumulation rate data versus platform duration intervals from Central Luconia Province (Figure 29).

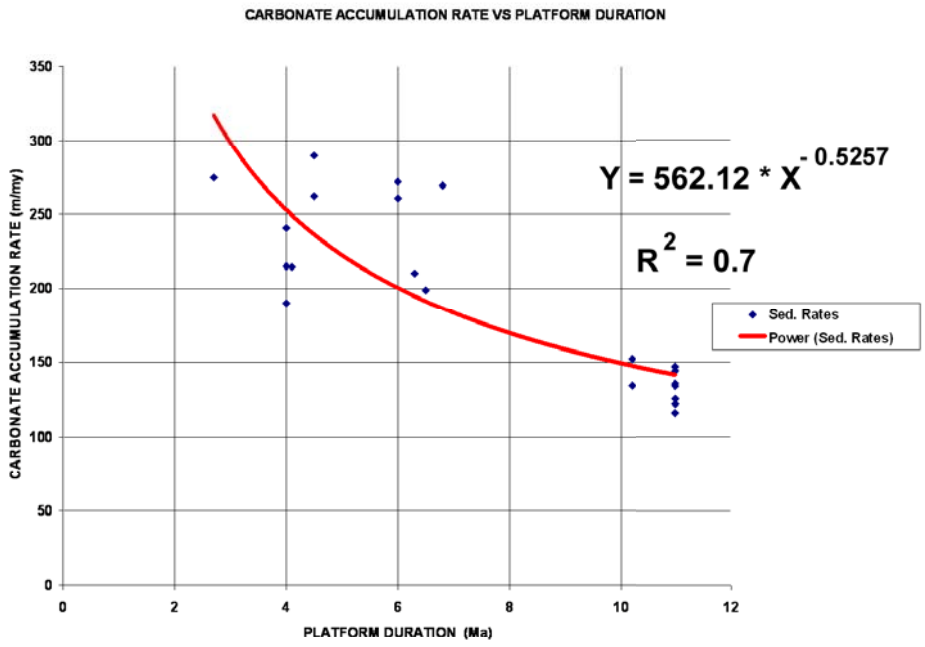

Figure 29. Graph of platform duration vs. carbonate accumulation rates with data from Table 11. According to the equation, accumulation rates are inversely proportional to the square root of time.

It is important to make clear that carbonate accumulation rates were underestimated because thicknesses were not corrected for compaction, and they also

prograded laterally while growing upward (aggradational to progradational growth patterns), which indicates that vertical growth was limited by available accommodation space rather than by growth potential of the platforms themselves.

If a carbonate platform under favorable conditions can grow at rates of 1,000-10,000 m/my (Kendall and Schlager, 1981; Schlager, 1981; Bosscher and Schlager, 1993), then rises of relative sea-level at rates 1,000-10,000 m/my may be required to drown healthy platforms. This range of sea-level rise rates is one to two orders of magnitude faster than sea-level rises reported by second and third-order cycles of Vail et al. (1977), therefore the drowning of carbonate platforms by a sea-level rise seems to be a paradox (Schlager, 1981; Wilson et al., 1998).

The high rate of sea-level rise required to drown a carbonate platform really limits the number of processes to be considered. However, additional factors accompanying sea-level rise can produce drowning, such as: environmental deterioration (Kendall and Schlager, 1981; Erlich et al., 1993; Schlager, 1981; Bice and Stewart, 1990; Hallock and Schlager, 1986; Vogt, 1989; Vecsei, 2003), high rate of sediment removal from platform tops (Schlager, 1981; Hine and Steinmetz, 1984; Bice and Stewart, 1990), higher-order sea-level rises superimposed over third-order cycles (Hine and Steinmetz, 1984; Schlager, 1981; Kendall and Schlager, 1981), and pulses in subsidence (Kendall and Schlager, 1981; Bice and Stewart, 1990).

Platforms in the Central Luconia Province were terminated by a combination of rapid third order sea-level rise along with environmental deterioration and rapid local subsidence in some areas. The environmental deterioration affected platforms gradually

from east to west as siliciclastics advanced westward, and was produced by the input of nutrients by terrestrial runoff of siliciclastic sediments from mainland Borneo. Nutrients may have stimulated the growth of plankton, which reduced the transparency of the water and decreased the carbonate growth potential of the platforms. Besides, many of these new organisms were bioeroders that destroyed reefal structures. Effects of nutrient influx might have extended beyond the range of active siliciclastic sedimentation (Hallock and Schlager, 1986, Erlich et al., 1993). Hence, platforms were possibly not suffocated by siliciclastics, instead they were terminated before the arrival of siliciclastics to their tops.

This study supports the hypothesis of platform termination by drowning. There is little evidence for subaerial exposure of platforms before each third-order sea-level rise (flooding events). However, the evidence from available seismic lines suggests that subaerial exposure affected some platforms during sea-level lowstands prior to final platform termination. However, if the platforms were exposed or not before termination is not an important factor because exposure preceding a sea-level rise will not significantly enhance the chances of drowning, even with the faster sea-level rises (Schlager, 1989).

Previous studies pointed out that carbonate platforms in the study area were drowned by relative sea-level rise that exceeded the rate of carbonate production (Epting, 1980, 1989). Vahrenkamp (1998) on the other hand suggested that sea-level fall and subaerial exposure terminated the platform growth. As explained before, no evidence was found for a subaerial exposure event associated with the demise of Central

Luconia platforms. This study supports in part the ideas of Zampetti et al. (2003) and Fulthorpe and Schlanger (1989), who suggested that drowning was caused by rapid sea-level rise along with environmental stress due to incoming siliciclastics. However, this study also supports an increased local subsidence coupled to rapid sea-level rise as the cause of drowning in places that were not affected by environmental deterioration.

Drowning in most of the platforms is characterized by a high-amplitude and low-frequency reflector at the platform tops. Such classical drowning unconformity is defined and discussed by Schlager (1981, 1989), and Schlager and Camber (1986). This unconformity marks the end of carbonate deposition and the beginning of deep-water sediments accumulation over the platform tops.

Another important point about drowning is that it was not coeval across the area. The first platforms that drowned were those that were under the influence of higher local subsidence and subjected to more environmental deterioration by siliciclastics. These platforms were drowned around 12.5-9.7 Ma, and represent the thinner carbonate accumulations in the area. Those platforms that were able to keep growing were located in areas of lower subsidence (northern area), and areas not affected by environmental collapse (central and northern areas). These platforms were drowned (~6.3-5.5 Ma) due to a rapid sea-level rise combined with subsidence and environmental stress that reached the area as siliciclastics prograded northward. These platforms represent the thicker accumulations in the area.

Comparison to East Natuna Basin Carbonate Platforms

In order to establish a point of comparison with other South East Asian carbonate provinces, this study provides a comparison between Central Luconia carbonates and East Natuna Basin carbonates. Results are the following:

1) East Natuna carbonates began to accumulate approximately at the same period of time (early Middle Miocene) as Central Luconia carbonates. However, carbonate accumulation in Central Luconia terminated around ~5.5 Ma (latest Late Miocene time), whereas carbonates on East Natuna Basin terminated around ~4.2 Ma (Early Pliocene time) in L-Structure (May and Eyles, 1985; Rudolph and Lehmann, 1989), and approximately ~3.8 Ma (Early Pliocene time) in Segitiga Platform (Bachtel et al., 2004).

2) Carbonate growth patterns in both carbonate complexes were dominated by the sea-level fluctuations and local and regional variations in subsidence across the area. These factors produced the coalescence of small platforms to form Segitiga Platform in East Natuna Basin at the end of Middle Miocene time. In the Central Luconia area coalescence of carbonate platforms are not visible in the seismic data available. Growth patterns in Central Luconia were also affected by an environmental stress accompanying siliciclastic influx, which was not observed in East Natuna Basin carbonates.

3) The termination of East Natuna carbonates was produced by the combined effect of rapid subsidence and sea-level rise at the end of Early Pliocene time, whereas carbonates on Central Luconia Province were drowned by the combined effect of rapid sea-level rise, high subsidence and environmental deterioration at the end of Middle Miocene time.

4) East Natuna Basin carbonates showed clear signs of karstification on the top of the carbonate sequence, therefore there was a subaerial exposure event immediately before platform termination. Central Luconia carbonates did not show evidence of karstification before platform termination.

5) After termination, both carbonate systems were covered by prograding siliciclastic sediments. The time gap between platform termination and the arrival of siliciclastic sediments to platform tops is unknown.

CHAPTER VI

CONCLUSIONS

Interpretation of the regional SEAS “Supertie” seismic survey, published data, and careful review of previous studies in the area, make it possible to analyze the evolution and demise of Middle to Late Miocene carbonate platforms in the Central Luconia Province. The main conclusions drawn from this study are:

1) Carbonate deposition in the Central Luconia Province began at ~16.5 Ma with the deposition of the third-order Cycle 2.3 (~16.5 Ma). Carbonate platforms were initiated on structural highs that were created by strike-slip, and to a lesser extent, extensional deformation during Oligocene to Early Miocene time.
2) Eustatic sea-level change, differential tectonic subsidence, regional flexural subsidence, and environmental deterioration by siliciclastic influx were the primary controls on platform evolution and stratal geometries. Five platform Growth Stages were identified across the study area, each separated by a sequence boundary.
3) Sedimentation rates estimated from Central Luconia carbonate platforms confirmed the decrease of carbonate accumulation rates with increasing platform duration. This trend, estimated over approximately ~10 Myr, followed the relationship of Schlager et al. (1998), who suggests that accumulation rates are proportional to the square root of time.

4) Siliciclastics influx from mainland Borneo probably introduced nutrients to offshore Borneo, which affected platforms beyond the range of active siliciclastic sedimentation. Nutrient excess disrupted the reef communities, resulting in decreased carbonate accumulation rates and increased rates of bioerosion.
5) Carbonate platforms drowned and then were covered by siliciclastic sediments, probably from the Baram Delta and the Rajang Flysch Belt. Although the time between drowning and siliciclastic influx to the platform tops is unknown, it was earlier in the southeastern part of the study area than in the northwestern part.
6) Carbonate platforms on Central Luconia Province were drowned at different times. The first platforms drowned were those subjected to intense subsidence, the sea-level rise and to effects of siliciclastic sediment influx. The second (and last) group of platforms drowned due to the combined effect of high local subsidence, rapid sea-level rise at the beginning of cycle 3.3, and environmental stress due to incoming siliciclastics.
7) Although in the seismic data used there is evidence of karst features during early lowstand periods, there is no evidence of subaerial exposure events prior to terminal drowning of platforms. This interpretation contrast with those of previous studies (Epting, 1980, 1989; Fulthorpe and Schlanger, 1989; Vahrenkamp, 1998, Zampetti et al., 2003; Vahrenkamp et al., 2004).

8) Growth Stage stratal geometries shown by carbonate platforms in the East Natuna Basin were affected by sea-level changes, and local variations in subsidence, whereas the Growth Stage stratal geometries in Central Luconia Province were affected by the same factors, plus an environmental deterioration, which produced a reduction of accumulation rates in the areas affected.
9) Carbonate accumulation in East Natuna Basin and Central Luconia Province was initiated approximately at ~16.5 Ma. Carbonate platform termination occurred first in Central Luconia Province (~5.5 Ma) and then in East Natuna Basin (~3.8 Ma).
10) East Natuna Basin carbonates show evidence of subaerial exposure immediately before platform termination. Central Luconia carbonate platform successions do not show exposure features prior to platform termination.

REFERENCES CITED

Ali, M. Y., 1994, Reservoir development in Miocene carbonates, Central Luconia Province, Offshore Sarawak: AAPG International Conference and Exhibition, Kuala Lumpur, Malaysia, p. 1134.

Bachtel, S. L., R. D. Kissing, D. Matron, S. P. Rahardjanto, P. A. Dunn, and B. A. MacDonald, 2004, Seismic stratigraphy evolution of the Miocene-Pliocene Segitiga Platform, East Natuna Sea, Indonesia: The origin, growth, and demise of an isolated carbonate platform, *in* G. P. Eberli, J. L. Masaferro, and J. F. Sarg, eds., Seismic imaging of carbonates reservoirs and systems: AAPG Memoir 81, p. 309-328.

Ben-Avraham, Z., and S. Uyeda, 1973, The evolution of the China basin and the Mesozoic paleogeography of Borneo: Earth and Planetary Science Letters, v. 18, p. 365-376.

Ben-Avraham, Z., 1978, The evolution of marginal basins and adjacent shelves in East and Southeast Asia: Tectonophysics, v. 45, p. 269-288.

Bice, D. M., and K. G. Stewart, 1990, The formation and drowning of isolated carbonate seamounts: tectonic and ecological controls in the northern Apennines: International Association of Sedimentologists Special Publication, v. 9, p. 145-168.

Bracco Gartner, G. L., W. Schlager, and E. W. Adams, 2004, Seismic expression of the boundaries of a Miocene carbonate platform, Sarawak, Malaysia, *in* G. P. Eberli,

J. L. Masaferro, and J. F. Sarg, eds., Seismic imaging of carbonate reservoirs and systems: AAPG Memoir 81, p. 351-365.

Briais, A. P., P. Tapponnier, and G. Pautot, 1989, Constraints of Sea Beam data on crustal fabrics and seafloor spreading in the South China Sea: Earth and Planetary Science Letters, v. 95, p. 307-320.

Briais, A., P. Patriat, and P. Tapponnier, 1993, Updated interpretation of magnetic anomalies and seafloor spreading stages in the South China Sea: Implications for the Tertiary Tectonics of SE Asia: Journal of Geophysical Research, v. 98, p. 6299-6328.

Bosscher, H., and W. Schlager, 1993, Accumulation rates of carbonate platforms: The Journal of Geology, v. 101, p. 345-355.

Daly, M. C., B. G. D. Hooper and, D. G. Smith, 1987, Tertiary plate tectonics and basin evolution in Indonesia: Proceedings Indonesian Petroleum Association, Sixteenth annual Convention, p. 399-428.

Daly, M. C., M. A. Cooper, I. Wilson, D. G. Smith, and B. G. D. Hooper, 1991, Cenozoic plate tectonics and basin evolution in Indonesia: Marine and Petroleum Geology, v. 8, p. 2-21.

England, P., and P. Molnar, 1990, Right-lateral shear and rotation as the explanation for strike-slip faulting in eastern Tibet: Nature, v. 344, p. 140-142.

Epting, M., 1980, Sedimentology of Miocene carbonate buildups, Central Luconia, offshore Sarawak: Bulletin of the Geological Society of Malaysia, v. 12, p. 17-30.

Epting, M. 1989, The Miocene Carbonate buildups of Central Luconia, offshore Sarawak, *in* A. W. Bally, ed., Atlas of seismic stratigraphy: AAPG Studies in Geology, v. 27, p. 68-173.

Erlich, R. N., S. F. Barrett, and G. B. Ju, 1990, Seismic and geologic characteristics of drowning events on carbonate platforms: AAPG Bulletin, v. 74, p. 1523-1537.

Erlich, R. N., A. P. Longo Jr., and S. Hyare, 1993, Response of carbonate platform margins to drowning: Evidence of environmental collapse, *in* R. G. Loucks and J. F. Sarg, eds., Carbonate sequence stratigraphy: AAPG Memoir 57, p. 241-266.

Fournier, M., L. Jolivet, P. Davy, and J-C Thomas, 2004, Backarc extension and collision: an experimental approach to the tectonics of Asia: Geophys. J. Int., v. 157, p. 871-889.

Fuller, M., R. Haston, J. L. Lin, B. Richter, E. Schmidtke, and J. Almasco, 1991, Tertiary paleomagnetism of region around the South China Sea: Journal of Southeast Asian Earth Sciences, v. 6, p. 161-184.

Fulthorpe, C. S. and S. O. Schlanger, 1989, Paleo-oceanographic and tectonic settings of Early Miocene reefs and associated carbonates of offshore Southeast Asia: AAPG Bulletin, v. 73, p. 729-756.

Gower, R. J. W., 1990, Early Tertiary plate reconstructions for the South China Sea region: constraints from northwest Borneo: Journal of Southeast Asian Earth Sciences, v. 4, no. 1, p. 29-35.

Hageman, H., 1987, Paleobathymetrical changes in NW Sarawak during Oligocene to Pliocene: Bulletin of the Geological Society of Malaysia, v. 21, p. 91-102.

Haile, N. S., M. W. McElhinny, and I. McDougall, 1977, Paleomagnetic data and radiometric ages from the Cretaceous of West Kalimantan (Borneo), and their significance in interpreting regional structure: Journal of the Geological Society of London, v. 133, p. 133-144.

Hall, R., 1996, Reconstructing Cenozoic SE Asia, *in* R, Hall, and J. Blundell, eds., Tectonic evolution of Southeast Asia: Geological Society Special Publications, London, Geological Society of London, p. 153-184.

Hall, R., 1997, Cenozoic plate tectonic reconstructions of SE Asia, *in* A. J. Fraser, S. J. Matthews, and R. W. Murphy, eds., Petroleum Geology of Southeast Asia: Geological Society Special Publications, London, Geological Society of London, p. 11-23.

Hall, R., 2002, Cenozoic geological and plate tectonic evolution of SE Asia and the SW Pacific: computer-based reconstructions, model and animations: Journal of Asian Earth Sciences, v. 20, p. 353-431.

Hallock, P., and W. Schlager, 1986, Nutrient excess and the demise of coral reefs and carbonate platforms: Palaios, v. 1, p. 389-398.

Hamilton, W., 1979, Tectonics of the Indonesian region: U. S. Geological Survey Professional Paper 1078: Reston, VA, U. S. Geological Survey, 345 p.

Haq, B. V., Hardenbol, J., Vail, P. R., 1988, Mesozoic and Cenozoic chronostratigraphy and eustatic cycles, *in* C. Wilgus, B. Hastings, C. Kendall, H. Posamentier, C. Ross, and J. van Wagoner, eds., Sea level changes: An integrated approach: SEPM Special Publications 42, p. 71-108.

Hine, A. C., and J. C. Steinmetz, 1984, Cay Sal bank, Bahamas – a partially drowned carbonate platform: Marine Geology, v. 59, p. 135-164.

Ho, K. F., 1978, Stratigraphic framework for oil exploration in Sarawak: Bulletin of the Geological Society of Malaysia, v. 10, p. 1-13.

Holloway, N. H., 1982, North Palawan Block, Philippines; its relation to Asian mainland and role in evolution of South China Sea: AAPG Bulletin, v. 66, p. 1355-1383.

Huchon, P., P. X. Le, and C. Rangin, 1994, Indochina Peninsula and the collision of India and Eurasia: Geology, v. 22, p. 27-30.

Hutchison, C. S., 1989, Geological evolution of Southeast Asia: Oxford Monographs on Geology and Geophysics, v. 13: Oxford, Clarendon Press, 368 p.

Hutchison, C. S., 2004, Marginal basin evolution: the southern South China Sea: Marine and Petroleum Geology, v. 21, p. 1129-1148.

Hutchison, C. S., 2005, Geology of North-West Borneo: Sarawak, Brunei and Sabah: Elsevier Academic Press, Amsterdam, The Netherlands, 421 p.

Karig, D. E., 1971, Origins and development of marginal basins in the western Pacific: Journal of Geophysical research, v. 76, p. 2542-2561.

Kearey, P., and M. Brooks, 1991, An introduction to geophysical exploration: Blackwell Science Publishing, Abingdon, Oxford, 254 p.

Kendall, G. St. C., and W. Schlager, 1981, Carbonates and relative changes in sea level: Marine Geology, v. 44, p. 181-212.

Lee, T. Y., and L. A. Lawver, 1992, Tectonic evolution of the South China Sea region: Journal of the Geological Society of China, v. 35, No 4, p. 353-388.

Lee, T. Y., and L. A. Lawver, 1995, Cenozoic plate reconstruction of Southeast Asia: Tectonophysics, v. 251, p. 85-138.

LePichon, X., M. Fournier, and L. Jolivet, 1992, Kinematics, topography, shortening, and extrusion in the India-Eurasia collision: Tectonics, v. 11, p. 1085-1098.

Longley, I. M., 1997, The tectonostratigraphic evolution of SE Asia, *in* A. J. Fraser, S. J. Matthews, and R. W. Murphy, eds., Petroleum Geology of Southeast Asia. Geological Society Special Publications, London, Geological Society of London, p. 311-339.

Ludwing, W. J., N. Kumar, and R. E. Houtz, 1979, Profiler-Sonobuoy measurements in the South China Sea Basin: Journal of Geophysical Research, v. 84, B7, p. 3505-3518.

Lumadyo, E., R. McCabe, S. Harder, and T. Lee, 1993, Borneo: A stable portion of the Eurasia margin since the Eocene: Journal of Southeast Asian Earth Sciences, v. 8, p. 225-231.

Mat-Zin, I. C., 1996, Tectonics evolution and sedimentation history of the Sarawak Basin: Bulletin of the Geological Society of Malaysia, v. 41, p. 41-52.

Mat-Zin, I. C., and R. E. Swarbrick, 1997, The tectonic evolution and associated sedimentation history of Sarawak Basin, eastern Malaysia: a guide for future hydrocarbon exploration, *in* A. J. Fraser, S. J. Matthews, and R. W. Murphy, eds., Petroleum Geology of Southeast Asia: Geological Society Special Publications, London, Geological Society of London, p. 237-245.

May, J. A., and D. R. Eyles, 1985, Well log and seismic character of Tertiary Terumbu carbonate, South China Sea, Indonesia: AAPG Bulletin, v. 69, p. 1339-1358.

Metcalfe, I., 1996, Pre-Cretaceous evolution of SE Asian terranes, *in* R. Hall, and D. J. Blundell, eds., Tectonic evolution of Southeast Asia: Geological Society Special Publications, London, Geological Society of London, p. 97-122.

Metcalfe, I., 1998, Paleozoic and Mesozoic geological evolution of the SE Asian region: multidisciplinary constraints and implications for biogeography, *in* R. Hall, and J. D. Holloway, eds., Biogeography and geological evolution of SE Asia: Backhuys Publishers, Leiden, The Netherlands, p. 24-41.

Molnar, P., and P. Tapponnier, 1975, Cenozoic tectonics of Asia: Effects of a Continental Collision: Science, v. 189, p. 419-426.

Morley, C. K., 2002, A tectonic model for the Tertiary evolution of strike-slip faults and rift basins in SE Asia: Tectonophysics, v. 347, p. 189-215.

Moss, S. J., J. Chambers, I. Cloke, A. Carter, D. Satria, J. R. Ali, and S. Baker, 1997, New observations on the sedimentary and tectonic evolution of the of the Tertiary Kutei basin, east Kalimantan, *in* A. J. Fraser, S. J. Matthews, and R. W. Murphy, eds., Petroleum Geology of Southeast Asia: Geological Society Special Publications, London, Geological Society of London, p. 395-416.

Packham, G. H., 1993, Plate tectonics and the development of sedimentary basins of the dextral regime in western Southeast Asia: Journal of Southeast Asian Earth Sciences, v. 8, p. 497-511.

Pautot, G., C. Rangin, A. Briais, J. Wu, S. Han, H. Li, Y. Lu, and J. Zhou, 1990, The axial ridge of the South China Sea: a seabeam and geophysical survey: Oceanologica Acta, Vol. 13, p. 129-143.

Peltzer. G., and P. Tapponnier, 1988, Formation and evolution of strike-slip faults, rifts, and basins during the India-Asia collision; an experimental approach: Journal of geophysical Research, B, Solid Earth and Planets, v. 93, p. 15085-15117.

Pupilli, M., 1973, Geological evolution of South China Sea area: Tentative reconstruction from borderland geology and well data, Proceedings of the Second Annual Convention, Jakarta, Indonesia: Indonesian Petroleum Association, p. 223-241.

Rangin, C., L. Jolivet, and M. Pubellier, 1990, A simple model for the tectonic evolution of Southeast Asia and Indonesia regions for the past 43 Ma: Bulletin of the Geological Society of France, v. 6, p. 887-905.

Rangin, C., M. Klein, D. Roques, P. X. Le, and L. V. Trong, 1995, The Red River fault system in the Tonkin Gulf, Vietnam: Tectonophysics, v. 243, p. 209-222.

Ru, K., and J. D. Pigott, 1986, Episodic rifting and subsidence in the South China Sea: AAPG Bulletin, v. 70, p. 1136-1155.

Rudolph, K. W., and P. J. Lehmann, 1989, Platform evolution and sequence stratigraphy of the Natuna Platform, South China Sea, *in* P. D. Crevello, J. L. Wilson, J. F. Sarg, and J. F. Read, eds., Controls on carbonate platform and basin development: SEPM Special Publication 44, p. 353-361.

Schlager, W., 1981, The paradox of drowned reefs and carbonate platforms: GSA Bulletin, v. 92, p. 197-211.

Schlager, W., and O. Camber, 1986, Submarine slope angles, drowning unconformities, and self erosion of limestone escarpments: Geology, v. 14, p. 762-765.

Schlager, W., 1989, Drowning unconformities on carbonate platforms, *in* P. D. Crevello, J. L. Wilson, J. F. Sarg, and J. F. Read, eds., Controls on carbonate platform and basin development: SEPM Special Publication 44, p. 15-25.

Schlager, W., D. Marsal, P. A. G. van der Geest, and A. Sprenger, 1998, Sedimentation rates, observation span, and the problem of spurious correlation: Mathematical Geology, v. 30, no. 5, p. 547-556.

Schlager, W., 1999, Scaling of sedimentation rates and drowning of reefs and carbonate platforms: Geology, v. 27, no. 2, p. 183-186.

Schmidtke, E. A., M. D. Fuller, and R. B. Haston, 1990, Paleomagnetic data from Sarawak, Malaysia Borneo, and the Late Mesozoic and Cenozoic tectonics of Sundaland: Tectonics, v. 9, p. 123-140.

Tapponnier, P., G. Peltzer, D. A. Y. Le, R. Armijo, and P. Cobbold, 1982, Propagating extrusion tectonics in Asia; new insights from simple experiments with plasticine: Geology, v. 10, p. 611-616.

Tapponnier, P., G. Peltzer, and R. Armijo, 1986, On the mechanics of the collision between India and Asia, *in* M. P. Coward, and A. C. Ries, eds., Collision Tectonics: Geological Society Special Publication 19, p. 115-157.

Taylor, B, and D. E. Hayes, 1980, The tectonic evolution of the South China Sea Basin, *in* D. E. Hayes, ed., Tectonic and Geologic evolution of southeast Asian seas and islands, part 1: American Geophysical Union Geophysical Monograph 23, p. 87-104.

Taylor, B, and D. E. Hayes, 1982, Origin and history of the South China Sea Basin, *in* D. E. Hayes, ed., Tectonic and Geologic evolution of Southeast Asian seas and islands, part 2: American Geophysical Union Geophysical Monograph 27, p. 23-56.

Tongkul, F., 1994, The geology of the northern Sabah, Malaysia: Its relationship to the opening of the South China Sea Basin: Tectonophysics, v.235, p. 131-137.

Vahrenkamp, V. C., 1998, Sr-isotope stratigraphy of Miocene carbonates, Luconia Province, Sarawak, Malaysia; implications for platform growth and demise and regional reservoir behavior, *in*: Anonymous, eds., AAPG 1998 annual meeting: Annual Meeting Expanded Abstracts – American Association of Petroleum Geologists, Tulsa, OK, United States: American Association of Petroleum Geologists and Society of Economic Paleontologists and Mineralogists, p. 1-7.

Vahrenkamp, V. C., F. David, P. Duijndam, M. Newall, and P. Crevello, 2004, Growth architecture, faulting, and karstification of a middle Miocene carbonate platform, Luconia Province, offshore Sarawak, Malaysia, *in* . P. Eberli, J. L. Masaferro, and J. F. Sarg, eds., Seismic imaging of carbonate reservoirs and systems: AAPG Memoir 81, p. 329-350.

Vail, P. R., R. G. Todd, and J. B. Sangree 1977, Seismic stratigraphy and global changes of sea level, part 5: chronostratigraphic significance of seismic reflections, *in* C. E. Payton, ed., Seismic stratigraphy – applications to hydrocarbon exploration: AAPG Memoir 26, p. 99-116.

Vecsei, A., 2003, Systematic yet enigmatic depth distribution of the world's modern warm-water carbonate platforms: the 'depth window': Terra Nova, v. 15, p. 170-175.

Vogt, P. R., 1989, Volcanogenic upwelling of anoxic, nutrient-rich water: a possible factor in carbonate-bank/reef demise and benthic faunal extinctions?: GSA Bulletin, v. 101, p. 1225-1245.

Wilson, M. E. J., and S. J. Moss, 1999, Cenozoic paleogeographic evolution of Sulawesi and Borneo: Palaeogeography, Palaeoclimatology, Palaeoecology, v. 145, p. 303-337.

Wilson, P. A., H. C. Jenkyns, H. Elderfield, and R. L. Larson, 1998, The paradox of drowned carbonate platforms and the origin of Cretaceous Pacific guyots: Nature, v.392, p. 889-894.

Zampetti, V., W. Schlanger, J-H van Konijnenburg and A-J Everts, 2003, Depositional history and origin of porosity in a Miocene carbonate platform of Central Luconia, offshore Sarawak: Bulletin of the Geological Society of Malaysia, v. 47, p. 139-152.

Zampetti, V., W. Schlanger, J-H van Konijnenburg and A-J Everts, 2004, Architecture and growth history of a Miocene carbonate platform from 3D seismic reflection

data; Luconia Province, offshore Sarawak, Malaysia: Marine and Petroleum Geology, v. 21, p. 517-534.

Zhou, D., K. Ru, and H. Chen, 1995, Kinematics of Cenozoic extension on the South China Sea continental margin and its implications for the tectonic evolution of the region: Tectonophysics, v. 251, p. 161-177.

VITA

Name:	Sergio Olave Hoces
Permanent Address:	5510 S. Rice Ave # 1614, Houston TX-77081
Email:	solave@geo.tamu.edu
Education:	B. S., Geophysical Engineering Universidad Simón Bolívar, Caracas, Venezuela (March 1998) M.S., Geology Texas A&M University College Station, TX 77843-3116, U.S.A. (August 2006)